

# Transition to turbulence in constant-mass-flux pipe flow

By A. G. DARBYSHIRE AND T. MULLIN

Department of Physics, University of Oxford, Parks Road, Oxford OX1 3PU, UK

(Received 9 February 1994 and in revised form 16 November 1994)

We report the results of an experimental study of the transition to turbulence in a pipe under the condition of constant mass flux. The transition behaviour and structures observed in this experiment were qualitatively the same as those described in previous reported studies performed in pressure-driven systems. A variety of jet and suction devices were used to create repeatable disturbances which were then used to test the stability of developed Poiseuille flow. The Reynolds number ( $Re$ ) and the parameters governing the disturbances were varied and the outcome, whether or not transition occurred some distance downstream of the injection point, was recorded. It was found that a critical amplitude of disturbance was required to cause transition at a given  $Re$  and that this amplitude varied in a systematic way with  $Re$ . This finite, critical level was found to be a robust feature, and was relatively insensitive to the form of disturbance. We interpret this as evidence for disconnected solutions which may provide a pointer for making progress in this fundamental, and as yet unresolved, problem in fluid mechanics.

---

## 1. Introduction

Since the original work of Reynolds (1883) on the transition to turbulence in a pipe of circular cross section, the subject has remained one of the most intriguing in fluid mechanics. Some of the reasons for the longevity of interest in this topic can be gleaned from Reynolds' original paper. First, he observed that as the flow rate was increased disordered motion initially arose in the form of patches of turbulent fluid separated by regions of ordered or laminar flow. This is quite counterintuitive since one might expect the whole flow field to become turbulent, rather than forming distinct patches. Secondly, Reynolds found two critical values of the ratio  $\nu/(U_m D_p)$ , where  $\nu$  is the kinematic viscosity,  $U_m$  is the mean flow velocity and  $D_p$  is the pipe diameter, for which the transition to turbulence occurred. The lower value was found when experiments were performed in a tightly controlled environment using precision equipment and the higher value was obtained using industrial pipes and the mains water supply. The inverse of Reynolds' ratio is what we now define to be the Reynolds number,  $Re$ , i.e.

$$Re = U_m D_p / \nu.$$

The critical ratios found by Reynolds correspond to a lower critical  $Re$  of 2260 and an upper critical  $Re$  of 12000. Further, Reynolds observed that if insufficient time was allowed between repetitions of the experiment, or if the tank was stirred, he did not get repeatable results in his 'controlled' experiments. Hence it can be assumed that the flow is susceptible to a finite-amplitude disturbance and that there is a lower critical  $Re$  of around 2000 below which all disturbances will decay. Subsequent series of

experiments have raised the maximum upper critical  $Re$  observed to a value in excess of  $10^5$  (Pfenninger 1961). However, the minimum lower critical value for transition to occur has remained close to the value obtained by Reynolds. Studies by Binnie & Fowler (1947), Lindgren (1958), Leite (1959) and Wygnanski & Champagne (1973) have placed it in the range  $1800 < Re < 2300$ .

The theoretical aspects of the problem have been investigated by several authors using linear and weakly nonlinear stability theory. The generally accepted conclusion is that Hagen–Poiseuille flow is linearly stable to infinitesimal axisymmetric perturbations and is also most likely to be stable to non-axisymmetric ones (see Drazin & Reid 1981; Stuart 1981 for discussions). Thus, in principle, laminar flow may be maintained at any Reynolds number providing extraneous disturbances are vanishingly small, which helps explain the large upper critical value of  $Re$  found by Pfenninger in his very well-controlled experiments. Therefore, attempts have been made to consider weakly nonlinear effects on the stability problem by Davey & Nguyen (1971), Itoh (1977) and Davey (1978). However, none of these studies produced conclusive evidence for the existence of finite-amplitude modes. More recently, Smith & Bodonyi (1982) identified neutral modes at high  $Re$  when the flow was modelled with a nonlinear critical layer and was subjected to three-dimensional disturbances. Further, Bergstrom (1993) considered combinations of the least-damped linearized eigenmodes and found that they could grow for a finite time before finally decaying.

Almost all of the experimental studies, including Reynolds' original work, have been concerned with the effects of natural or induced disturbances initiated in the inlet region of the pipe. Attention is then focused on the structure of the turbulent patches and the transition process which gives rise to them. For example, Lindgren (1958) and Bandyopadhyay (1986) placed orifice plates and obstacles in the pipe inlet in their flow visualization work. Thus both the mean flow field and the disturbances themselves evolve as they progress downstream. This is of course different to the situation considered in the theoretical work discussed above which is concerned with the stability of Poiseuille flow. However, the stability of the inlet flow was investigated theoretically by Tatsumi (1952) and later extended by Smith (1960) and it was shown that this flow is linearly unstable for  $Re > 9700$ .

The most extensive experimental study of transition in a pipe was performed by Wygnanski and co-workers in the 1970s. Wygnanski & Champagne (1973, hereafter referred to as WC73) conducted a meticulous study of the structures and phenomena associated with transitional and turbulent pipe flow in the  $Re$  range 1000–50 000. They identified two transitional flow states, the type observed being dependent on  $Re$ . For  $2000 < Re < 2700$  the transition structures were termed 'turbulent puffs'. These flow structures have a well-defined upstream (rear) interface between a localized region of disordered 'turbulent' fluid and the laminar fluid following on behind. This interface is sharp in the centre of the pipe and is advected along at a speed just less than the mean flow rate of the fluid. Ahead of the region of disordered motion are larger-scale structures which form an indeterminate downstream (front) interface with undisturbed laminar fluid ahead of the puff. These features are described by Coles (1981) in the context of 'coherent structures' in fluid flows.

The second transitional state is found at  $Re > 3500$  and consists of structures termed 'turbulent slugs' separated by regions of laminar flow. These are observed to have well-defined interfaces at both ends and extend over almost the whole pipe cross-section. When  $Re$  is large ( $> 10000$ ) the speeds of the front and rear interfaces approach  $1.5U_m$  and  $0.5U_m$  respectively. As a consequence, the region of turbulence increases in size as the slug is advected along the pipe, whereas in the case of turbulent puffs the spatial

extent of the highly disordered motion grows much less quickly. This feature of turbulent puff structures was investigated in a later paper by Wagnanski, Sokolov & Friedman (1975, hereafter referred to as WSF75) where the concept of an 'equilibrium puff' was introduced. These are structures with the characteristics of turbulent puffs which neither grow in spatial extent or split into more than one turbulent puff as they advect downstream. Equilibrium puffs were found to occur in the range  $2100 < Re < 2400$ . The distinction was based largely on the criterion of splitting due to the indeterminate nature of the downstream (front) interface of the turbulent puff. The highly disordered interior section between the two interfaces for turbulent slugs is indistinguishable from that seen in fully developed turbulent pipe flow which is not the case for turbulent puffs. In the latter case the disordered flow contains large-scale structures as discussed above.

The stability of fully developed Poiseuille flow was studied by Leite (1959). He followed the ideas of Schubauer & Skramsted (1947) who investigated the stability of the boundary layer over a flat plate by adding a small oscillatory perturbation to the flow. Leite introduced small axisymmetric disturbances into the flow by oscillating an elastic membrane at the pipe wall and found that they decayed at a rate suggested by linear stability theory. However, larger disturbances produced by a ring aerofoil in the centre of the pipe were observed to grow into turbulent patches. This latter experimental device was refined by Fox, Lessen & Bhat (1968) who found that above  $Re = 2150$  the flow was unstable to a small azimuthally periodic disturbance at certain frequencies.

In all of the above studies, the perturbation was always present in the flow field. This can lead to complications in the interpretation of the results because it is not always clear whether the transition occurs as the result of cumulative effects on the flow or as a discrete event in response to the disturbance. In addition, multiple regions of turbulence separated by laminar flow are sometimes observed in pipe flows with a continuous disturbance source, which led Rotta (1956) to use the term intermittency to describe the dynamics of the flow.

In order to overcome this potential difficulty WSF75 introduced a single pulse disturbance into the inlet flow to induce transition. Thus, in this case, only one transition event was present in the pipe at any given time. The idea was that an ensemble average of turbulent puffs could be then collated, avoiding the problems associated with disturbances at various stages of development or decay interacting with each other. The averaging was achieved using the sharp rear interface to synchronize the recordings of successive turbulent puffs as the radial and streamwise measuring positions were varied. These measurements were then used to build a representation of the flow field across the whole pipe and thus to expose the internal structure of the puffs.

The above investigation was extended by Rubin, Wagnanski & Hartonidis (1980) who investigated the effects of introducing single pulse disturbances into fully developed Poiseuille flow. One important observation they made was that the structure of the transitional flow does not depend on the method of production, i.e. if the disturbance added to Poiseuille flow is large enough to cause transition then the downstream outcome is the same as that produced by a disturbed inlet.

Our study follows on from the work reported in Rubin *et al.* (1980) to the extent that we examine in detail and give quantitative results for the effects of introducing various types of single disturbances into developed Poiseuille flow. Unlike all previously reported investigations we use a rig where the flow is driven by a displacement device so that there is a constant mass flux and hence constant  $Re$  irrespective of the flow

conditions in the pipe. Details of the experimental rig and measuring techniques are given in §2 which is followed by an overview of the main findings in §3. A detailed discussion of the response of the flow to various forms of disturbance is presented in §4 and the evolution of individual perturbations is described in §5. The results of a study of the lower critical values of  $Re$  required to sustain turbulence are discussed in §6 and this is followed by an investigation into the relaminarization process in §7. Finally, we draw some conclusions in §8 and indicate new directions for study of this classical problem.

## 2. Experimental details

A schematic diagram of the apparatus is shown in figure 1. The pipe is constructed from individually machined sections of the Perspex which are push-fitted together and butted flush so that there is no measurable gap between each join. The pipe is manufactured in this way to ensure a uniform cross-section over its entire length. The joins do not disturb the flow and evidence for this is provided by the fact that the flow remains laminar at the maximum available Reynolds number of  $Re \approx 17000$  when no external disturbances are added. The internal diameter of the pipe  $D_p$  is  $20 \pm 0.01$  mm and each section is 158 mm in length with a wall thickness of the tube of 6 mm which ensures a rigid construction. The sections are held together on a metal base so as to form a total pipe length of 3800 mm or  $190D_p$ . At one end of the pipe there is a Perspex tank which holds approximately 28 l of water and is covered by a loose fitting lid. The pipe is connected to the supply tank via a smooth trumpet shaped inlet, as shown in figure 2(a), for most of the experiments. This device helps accelerate the development of Poiseuille flow and ensures a laminar flow over the whole Reynolds number range investigated for a flow which is initially disturbance free. On the other hand a sharp cornered inlet induces transition spontaneously at a Reynolds number of around 2000.

The fluid was pulled through the pipe by a cylindrical piston system. The piston is propelled by a reciprocating bearing on a ground leadscrew which is driven by a high-quality d.c. electric motor. The piston is counterbalanced in its housing by external weights hanging on pulleys. It is sealed by two neoprene piston rings which are covered by Teflon tape providing both a watertight seal and a sliding bearing surface. The piston itself is spray coated with Teflon to reduce friction at the seal and is supported at the front on two Teflon-coated feet. The entire piston and drive arrangement is mounted on a machined cast ALUMAX base. This material was selected because of its temperature stability.

The motor is driven at a constant speed using preset d.c. levels and the mechanism described ensures that the piston is withdrawn from its housing at a constant rate. This in turn leads to fluid being pulled from the tank through the pipe into the chamber at a constant volume flow or, since the fluid is incompressible, mass flux rate. Hence, even if the fluid in the pipe becomes turbulent the mass flux driven through the pipe will be unaffected and therefore the Reynolds number remains constant. The drive motor is fitted with a servo control system which allows its speed to be held constant to better than 0.5%. The environment in the laboratory was controlled by an air-conditioning system to limit long-term ambient temperature variations to within 1 °C of a mean temperature of 17 °C. Since there is a large thermal mass of fluid in the apparatus this control provided good short-term temperature stability. The actual temperature of the fluid was recorded to within 0.1 °C using a mercury thermometer placed in the tank. The control of the motor speed and the temperature gives the experiment an accuracy in  $Re$  of  $\pm 15$  at  $Re \approx 2000$ .

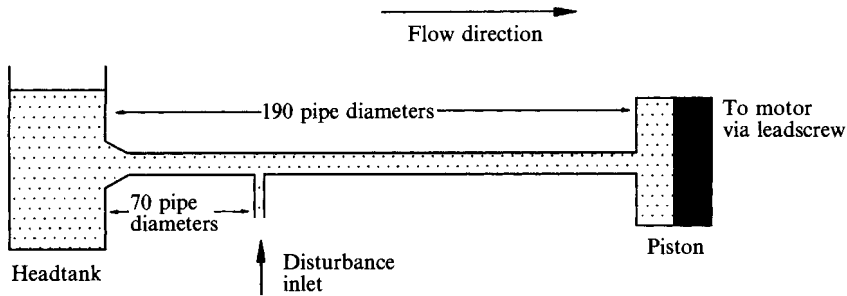


FIGURE 1. Schematic diagram of flow rig.

A forward-scatter laser Doppler velocimetry (LDV) system is used to make velocity time series measurements of the axial velocity component at a single point within the flow. The water is seeded with  $1\ \mu\text{m}$  latex beads which act as scatterers for the incident HeNe beams. The measuring region is  $0.35\ \text{mm}$  long so that the axial flow component is averaged over 2% of the tube diameter. The Doppler signal is processed using a commercial burst counting system which provides a continuous velocity versus time record. This was then sampled and stored on a Masscomp computer where further processing could be carried out. The flow was also studied using the flow visualization techniques of injecting dye and adding suspensions of anisotropic light-reflecting flakes to the fluid. In each case these were used to identify flow structures, and both still photographs and video recordings were made.

The stability of the basic laminar flow was investigated by injecting disturbances into the flow at a position along the length of the pipe where the flow was considered to be fully developed. Since the pipe is  $190D_p$  long the injection point was placed  $70D_p$  downstream of the pipe inlet in order that the evolution of any transitional flow structures produced could be followed. This distance is less than one might calculate to get 95% development of Poiseuille flow at  $Re \approx 2000$ , but the fluting of the inlet reduces the entrance length. The use of the term 'fully developed flow' implies that  $U_{axis} \approx 2U_{mean}$ , and a percentage qualification means that  $U_{axis} = n\%$  of  $2U_{mean}$ . LDV measurements on the central axis of the pipe showed that the flow was at least 94% developed at  $70\ \text{pipe diameters}$  downstream of the inlet for  $Re = 2200$  which is in the middle of the range of most of our experiments. A velocity profile was measured at  $70D_p$  and is shown in figure 2(b) along with a profile calculated from the known imposed flow rate. It can be seen that the profile is developed over most of the cross-sectional area of the pipe, but that the flow in the axial region of the pipe is slightly retarded. This is in agreement with work by Smith (1960) on the development of the parabolic profile.

In addition, we also checked our estimates by taking measurements at several points downstream beyond the distance where fully developed flow is assured (see for example Fargie & Martin 1971). The disturbance point was also moved further downstream but it was found to have no measurable effect on the observations other than limiting the time available for the development of disordered flow. Clearly, when  $Re$  is increased to a value well above the range 2000–2500 then the flow is not fully developed but, as we shall show, our results suggest that the details of the flow field in the centre of the tube do not appear to have a significant effect on the transition process.

The disturbances are derived from the motor and piston arrangement shown in figure 3(a). The generator consists of a disk onto which is fixed another disk of smaller diameter; the large disk is rotated by the motor through a gearbox at a fixed frequency

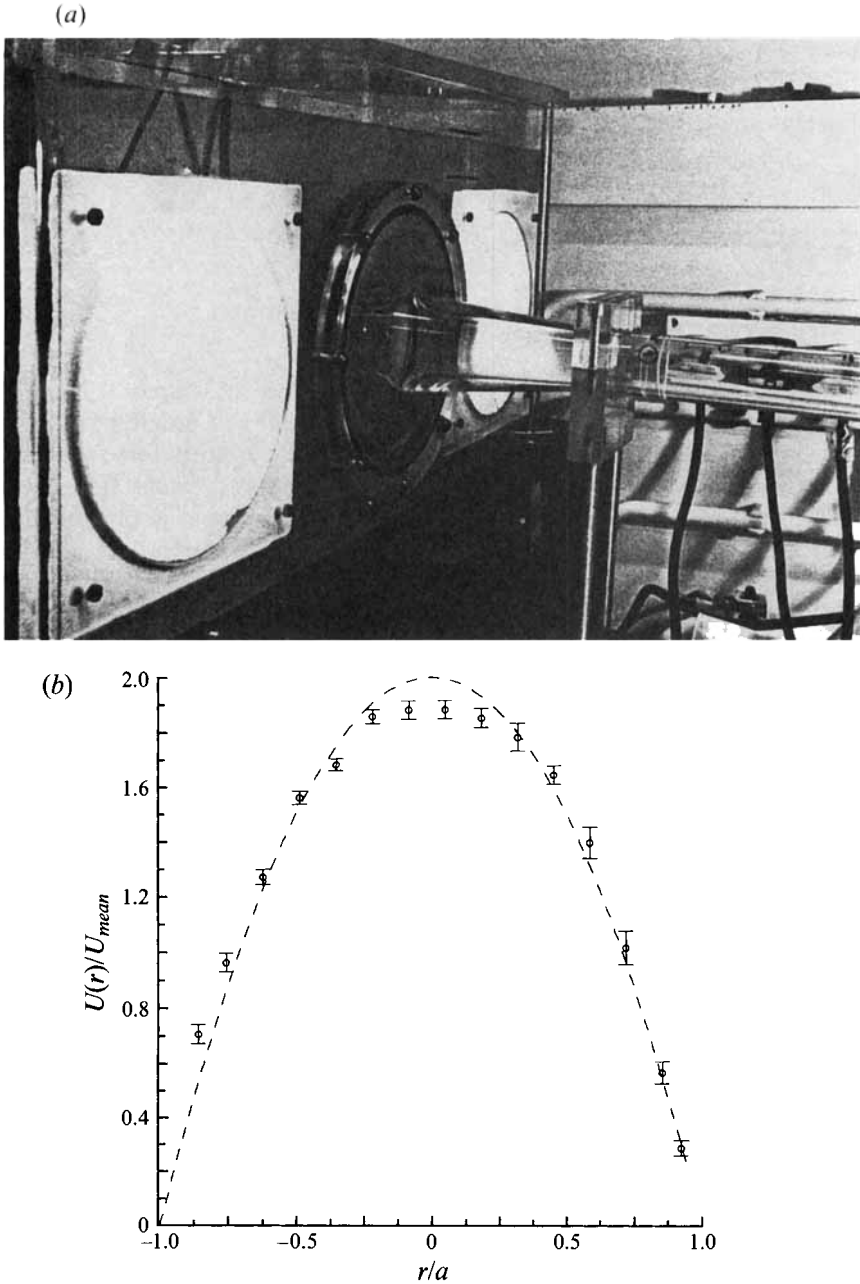


FIGURE 2. (a) Photograph of trumpet inlet to the pipe. (b) Measured velocity profile of laminar pipe flow  $70D_p$  from the pipe inlet at  $Re = 2210$ . The dotted line is the calculated Poiseuille profile.

$\omega$ . The actual frequency is measured using an attached shaft encoder. The piston is pushed forward by the small disk as the large one rotates, as indicated in figure 3(a). This motion drives a small piston which injects fluid into the pipe via tubes which lead to the disturbance inlet. A spring is used to help prevent the piston overshooting and return the piston to its original position after the initiation of a disturbance. A valve at the outlet of the device stops fluid being sucked out of the pipe on the return stroke

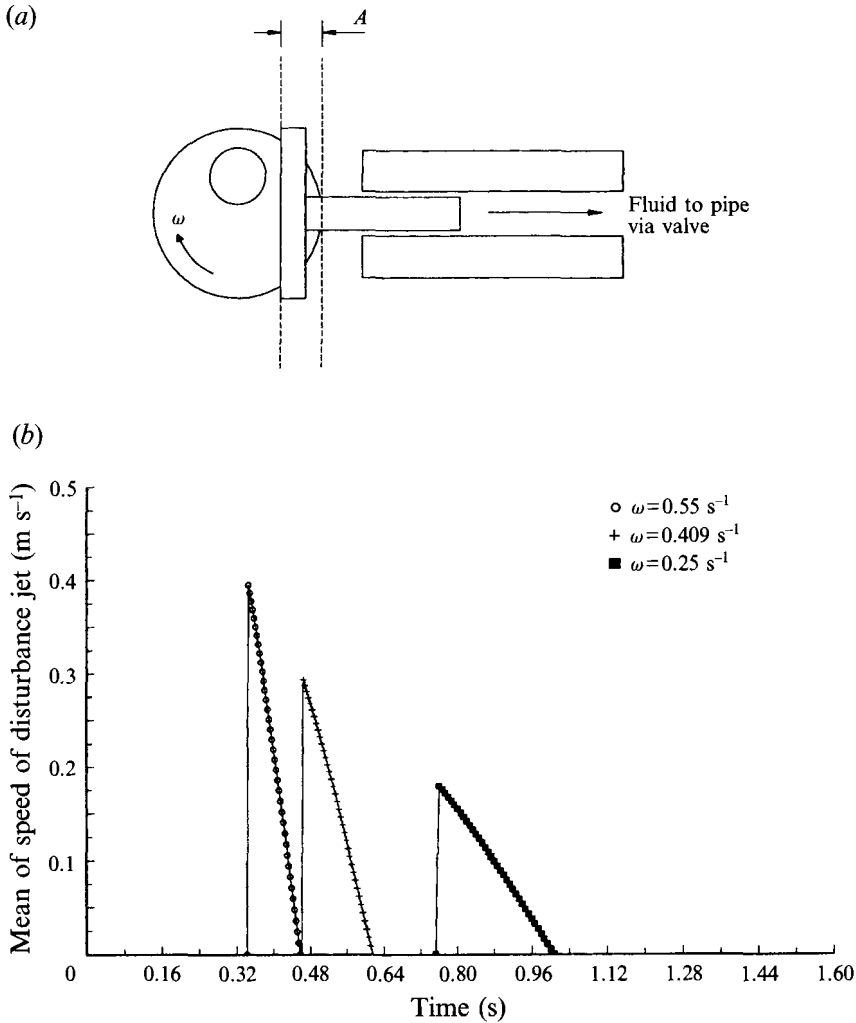


FIGURE 3. (a) Schematic diagram of disturbance generator. (b) Mean jet velocity plotted against time for the single-jet disturbance, amplitude 1.5.

of the piston. The maximum amplitude of the disturbance is taken to be the distance  $A$ , the travel of the piston. The speed of the piston is not constant over the stroke and a typical velocity against time plot is shown in figure 3(b). Since  $A$  is small with respect to the diameter of the large disk this velocity–time characteristic is linear after the initial impulse.

The form of the disturbance can clearly be changed by designing suitable inlet geometries. The two disturbance inlet geometries used in the experiments are shown in figure 4. In the first, the disturbance at the pipe is in the form of a single jet injected orthogonal to the main flow through a 2 mm diameter hole as shown in figure 4(a). The second system, shown in figure 4(b), involves an arrangement of valves and tubes which are used to produce multiple jets of diameter 0.5 mm directed azimuthally to the pipe flow so as to introduce a component of swirl into the main flow field. Both of the above disturbances in principle affect the flow everywhere since the fluid is incompressible. Therefore the multiple jet arrangement was also used to simultaneously inject and extract fluid from alternate azimuthal inlets in an attempt to

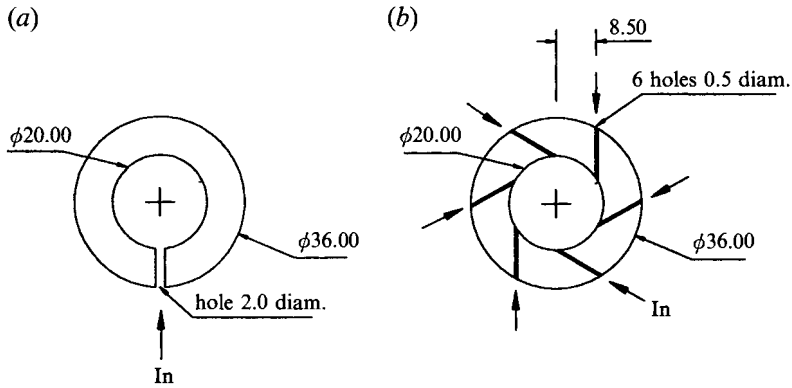


FIGURE 4. Disturbance geometries: (a) single jet, (b) six jet. All dimensions are in mm.

Reynolds number	2200
Disturbance amplitude	2.0
Disturbance frequency	$0.4 \text{ s}^{-1}$
Mean flow speed	$0.12 \text{ ms}^{-1}$
Maximum flow speed	$0.24 \text{ ms}^{-1}$
Maximum mean jet speed	$0.35 \text{ ms}^{-1}$
Duration of disturbance	0.1 s
Ratio of mass fluxes jet/mean flow	0.01

TABLE 1. Typical values of parameters in the experiments

localize the disturbance. Finally, some runs were carried out where the disturbance to the parabolic profile was provided by the extraction of fluid from the single jet inlet arrangement.

Only one disturbance event was created for each run of the experiment. The two parameters  $A$  and  $\omega$  along with the diameters of the inlets to the pipe characterize the disturbances in terms of the average flow rate of the disturbance and total mass flux added to the main flow. The generator arrangement had the advantage of being mechanically repeatable, i.e. for a given disturbance inlet configuration the total fluid injected and mean disturbance flow rate could be controlled using the two parameters, and then repeated when necessary. We present typical values of these parameters for both jet disturbance configurations in table 1. The units used for  $A$  throughout paper can be converted into millimetres by multiplying by 1.62.

It can be seen in table 1 that the mass flux of the disturbance is small when compared with that of the main flow. However, the initial mean flow speed of the injected jet is greater than the mean flow speed in the pipe at  $Re = 2200$  which is approximately mid-range for the majority of the experiments. Also, as will be shown below, the disturbed flow field is initially localized close to the inlet due to the short duration of the injection. Thus an estimate can be made of the distance travelled downstream before decay of those disturbances which do not cause transition.

The experimental arrangement described above means that each experiment is a 'single shot'. The transient time at both the beginning and the end of each run is approximately 10 s and is independent of  $Re$ . We show in figure 5 a typical measurement of the axial velocity close to the central axis of the pipe measured using the LDV system over the duration of one run of the experiment at  $Re = 2316$  to

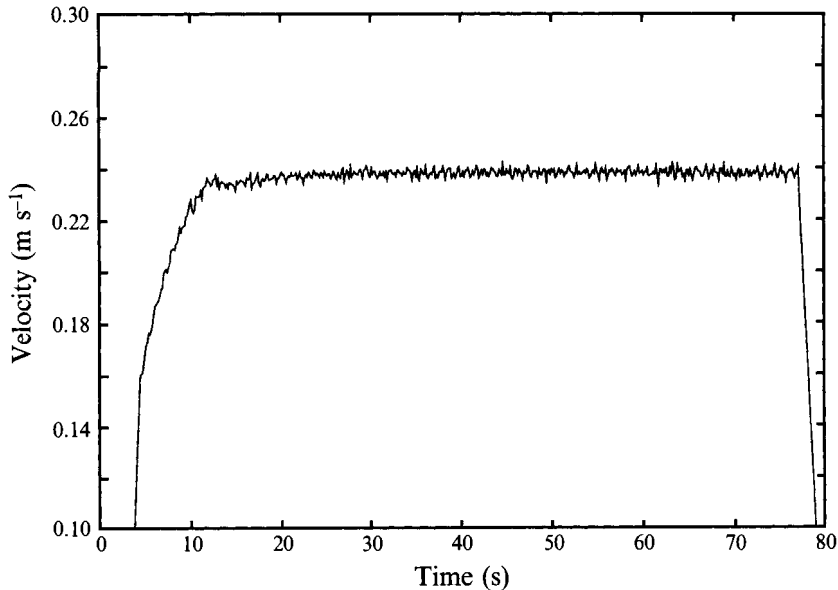


FIGURE 5. Velocity time trace of a typical experimental run,  $Re = 2316$ . The noise on the trace comes from the LDV system.

illustrate the transient effect at the beginning and end of each run. The useful experimental time available on each run is thus limited by the finite travel of the piston and is dependent on the motor speed. For example, at  $Re \approx 2200$  the useful experimental time is 60 s. After each run of the experiment the fluid is pushed back through the pipe into the tank and allowed to settle for a period of at least 30 minutes before the next run. This period was chosen empirically on the basis of flow visualization observations of the fluid in the tank and it was also found to be the minimum time required to give repeatability in the disturbance experiments. Finally, in all the experiments, the disturbance was only added after the starting transient in the flow had decayed away.

### 3. An overview of the results

In this section we present an overview of the experimental results and compare and contrast their general features with those reported in previous studies. Our aim is to see if there is any qualitative difference between the results for pressure-driven systems and our constant-mass-flux experiment. We choose the following particular sources for comparison: the flow visualization photographs of Bandyopadhyay (1986) and Lindgren (1958) and the axial velocity records obtained from hot-wire probes given in WC73 and WSF75.

The main features of our experimental results may be summarized as follows:

(i) Turbulent structures could be induced in the laminar flow in a controlled way by injecting a prescribed disturbance or in an *ad hoc* manner by stirring the supply tank or using a sharp flow inlet.

(ii) In the transitional region, the disordered flow was spatially localized in the pipe in the same way as reported in all previous studies in pressure-driven systems. It is sometimes argued that the relaminarization of the flow behind the disordered region is due to a drop in Reynolds number to a value which is insufficient to sustain

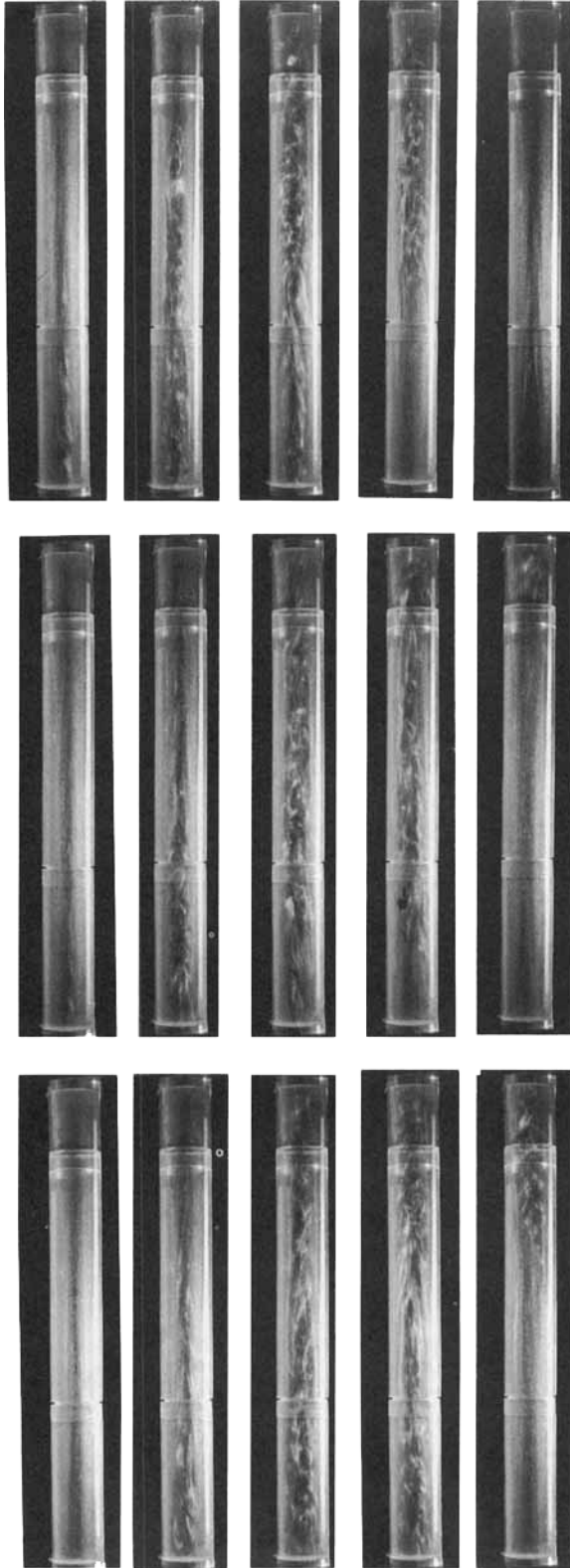


FIGURE 6. Flow visualization photographs showing the passage of an equilibrium puff at  $Re = 2200$ . The sequence starts in the top left corner and runs in the left to right rows.

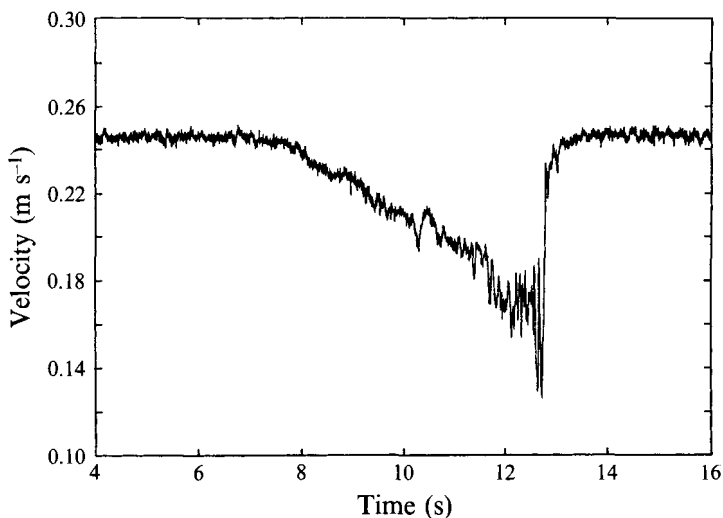


FIGURE 7. Velocity time trace of an equilibrium puff measured on the pipe axis using LDV,  $Re = 2300$ .

turbulence (see for instance Tritton 1988). Since, in our case, the Reynolds number is held constant, these physical arguments are inadequate to explain the relaminarization in our case.

(iii) There is a minimum value of  $Re$  below which the turbulent structures cannot be sustained. In our case we found this value to be in the range  $Re \approx 1760$ . Thus, no matter how large a disturbance was injected into the flow or how disturbed the fluid in the tank was, no non-decaying turbulence was observed. We studied this lower limit in detail using injected disturbances at  $Re \approx 1800$  and a discussion of the findings is given below in §6.

(iv) At values of Reynolds number greater than 1800 the introduction of a large enough disturbance into the flow produces a sustained transition to turbulence. Consider first Reynolds numbers just above this limit, e.g.  $Re \approx 2200$ . A typical well-developed structure is shown in the sequence of flow visualization photographs presented in figure 6. Here, transition was induced 'naturally' using the sharp pipe inlet from the supply tank. The pictures were taken  $140D_p$  from the inlet. We also show in figure 7 a typical LDV record taken of a similar event but now induced by an injected disturbance with the fluted inlet at the pipe entrance. The measurement point was close to the central axis of the pipe and located  $100D_p$  from the disturbance inlet. There is no observable qualitative difference between developed structures produced by injected jets and those induced naturally by the sharp flow inlet. The sequence of events as the structure is advected past the measurement point or camera can be interpreted as follows:

- (a) laminar flow;
- (b) a gradual reduction of the axial velocity in the centre of the pipe which can be seen directly on the LDV trace in figure 7;
- (c) helical wave-like structures are observed in the central axial part of the flow;
- (d) a highly disordered 'turbulent' region of fluid which covers the whole cross-section of the pipe;
- (e) a sharp interface with laminar flow upstream of the highly disordered region;
- (f) laminar flow.

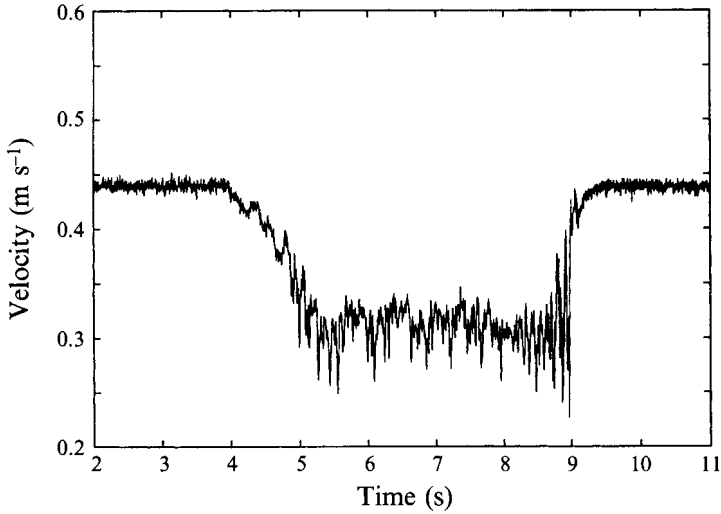


FIGURE 8. Velocity time trace of slug flow measured on pipe axis using LDV,  $Re = 4260$ .

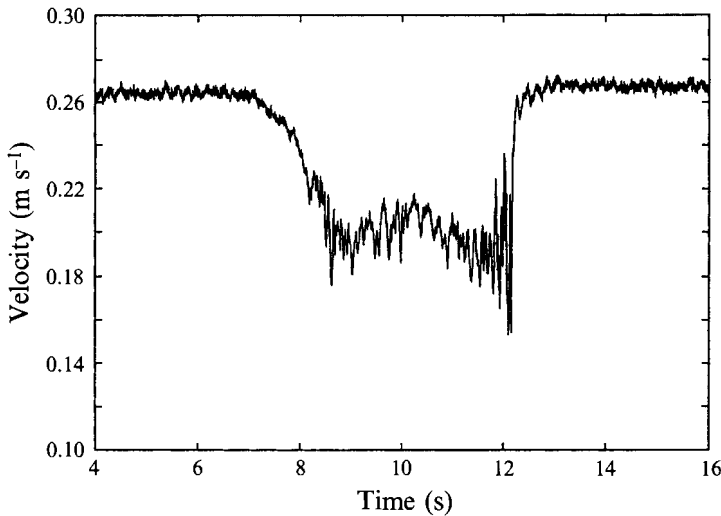


FIGURE 9. Example of flow which shows turbulent slug characteristics at low Reynolds number ( $Re = 2490$ ).

The upstream interface was observed to travel at a speed close to the mean flow speed. The above results from our constant-mass-flux device are consistent with and remarkably similar to those observed in the pressure-driven systems. Explicit comparison may be made between the LDV trace shown in figure 7 and figure 5 of WC73, and the flow visualization photographs given in figure 6 and those presented in figure 2 of Bandyopadhyay (1986). As discussed in the introduction, WC73 named this type of locally disordered flow a 'turbulent puff'.

(v) As the Reynolds number is increased stages (b) and (c) in (iv) above become less distinct and the structure develops a sharper downstream interface. A typical LDV measurement of the axial velocity for  $Re = 4240$  recorded  $100D_p$  from the disturbance inlet is shown in figure 8. The downstream interface becomes more pronounced as  $Re$

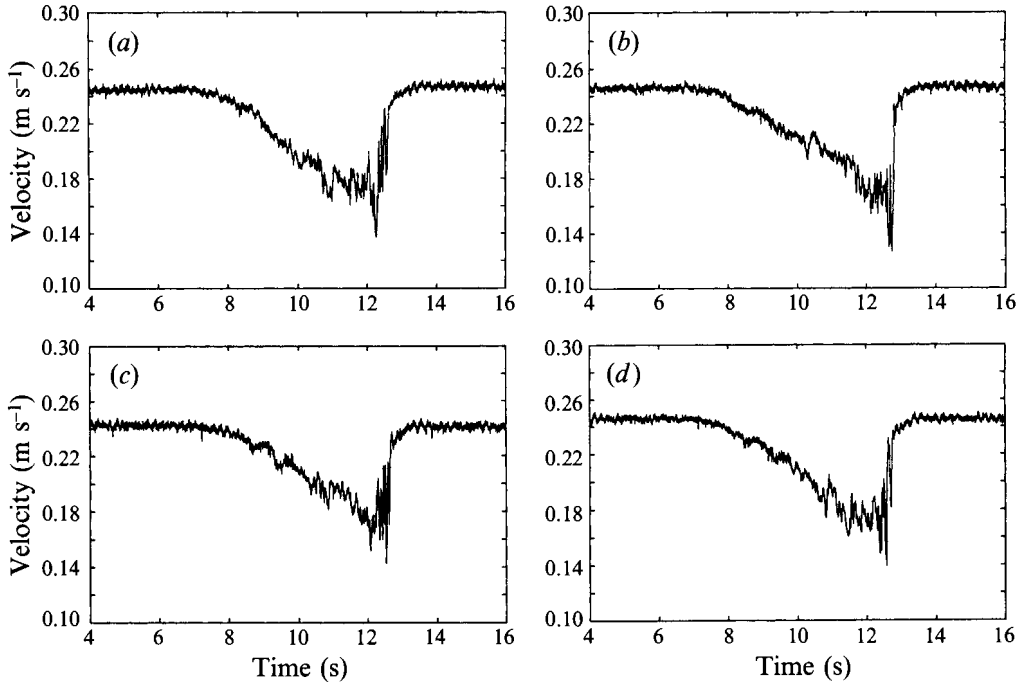


FIGURE 10. Velocity time traces of four different equilibrium puffs generated under constant experimental conditions ( $Re = 2269$ ).

is further increased, until a point is reached where the structure produced is a region of highly disturbed fluid separated by sharp interfaces from laminar fluid upstream and downstream. This structure was described as a ‘slug’ in WC73. However, in the boundary range of  $Re$  between the two flow types it is often difficult to distinguish between them. As an example consider the LDV trace shown in figure 9 recorded at  $Re = 2490$  and with the disturbance parameters at the same values as used in figure 7. Qualitatively the record has characteristics similar to the trace shown in figure 8 recorded at  $Re = 4240$  which is well into the slug regime, rather than the puff flow shown in figure 7. This is maybe an extreme instance but is an illustration of the point.

The above schematic descriptions of events glosses over some informative detailed behaviour of the flow. In the case of turbulent puffs, the relative size and distinctiveness of the regions within the puff varies quite markedly between repetitions of the experiment. This is true even if the Reynolds number and disturbance parameters are kept constant. A demonstration of this feature is provided by the results presented in figure 10. Here we show the velocity time traces for four repeated runs of the experiment. The disordered flow is a puff produced by a single jet disturbance with amplitude  $A = 1.7$  at  $Re = 2270$  and time is measured from the start of the injection of the disturbance. It can be seen that while the overall length and intensity of the non-laminar region is approximately the same in all four cases, the details of the time traces are quite different. In particular, the trailing edges contain very different numbers of sharp oscillations and the helical waves at the leading edge are not evident in figure 10(a). These differences in the details of the structure between realizations may partly be a consequence of having a single-point measurement of a flow field which is developing both spatially and temporally. However, this cannot explain the different number of large oscillations at the rear of the puff, for example. Thus we interpret the

differences as evidence for multiplicity of states in the transition process, which is a common feature of fluid flows (Benjamin 1978; Joseph 1981; Madden & Mullin 1994).

The feature of turbulent puffs which is most consistent is the time taken for the upstream interface to advect from the injection point to the LDV measurement station. For a set of 28 measurements taken at the above parameter values this time is  $11.9 \pm 0.2$  s which corresponds to a rear interface speed of  $0.95 \pm 0.03 U_m$  where  $U_m$  is the mean flow speed of the fluid in the pipe. This result is consistent with previous work (WC73, WSF75), when allowance is made for the fact that our measurement includes a growth phase of the turbulent structure whereas the earlier results are based on two-point measurements of a developed structure. The speeds of the front and rear interfaces of turbulent slugs were also measured; again these were found to be consistent with the measurements reported in previous works (WC73; Tritton 1988, figure 18.7). At  $Re = 9990$  we measured the speeds of the rear and front interfaces to be, respectively,  $0.57 \pm 0.05 U_m$  and  $1.39 \pm 0.1 U_m$ .

To summarize: the structures observed in transitional pipe flow in a constant-mass-flux device are qualitatively the same as those observed in a pressure-driven system. The overall size and speed of propagation of the regions of disordered flow is well-defined for repetitions of the experiment at the same parameter values. However, the details of the motion inside the turbulent region varies from run to run. Finally, the rear laminar/turbulent interface is not dependent on a local Reynolds number which drops below a critical threshold as is sometimes assumed in the discussion of the results from pressure-driven systems.

#### 4. Induction of transition using prescribed disturbances

As discussed above, the bulk properties of the developed flow structures appear to be independent of the details of the manner in which they are produced. However, we wish to carry out a systematic study of the initial phase of the transition process and so this part of the experiment involved the use of repeatable prescribed disturbances. In particular, we investigated the relationship between the size of the disturbance and the downstream outcome and also measured the time and length scales over which the turbulent structure developed. The method chosen was to add a controlled and repeatable disturbance to developed Poiseuille flow and then observe the downstream evolution of the flow. It is well known that even simple nonlinear systems can give very different outcomes for slight variations in initial conditions. Thus one might expect extreme sensitivity to the details of the disturbance injected into the flow. However, as we show below, the outcome of each experimental run for a given set of disturbance parameters seems to be insensitive to the exact form of the perturbation added to the flow.

We shall concentrate on Reynolds numbers at and just above the minimum for which transition is sustained because if there is a mechanism of instability one might expect this to be dependent on  $Re$  and have a minimum growth rate at the instability threshold. This should make it easier to identify any intermediate stages between the laminar and turbulent states (cf. Tollmein–Schlichting waves in boundary layers – for example, see the elegant work of Gaster 1990).

We then extend our investigations to higher Reynolds numbers to see if any differences become apparent in the transition process. These results are described at the end of this section where we present results for  $Re$  up to 10000. It is found that a finite amplitude of disturbance is still required for transition and localized slugs are formed.

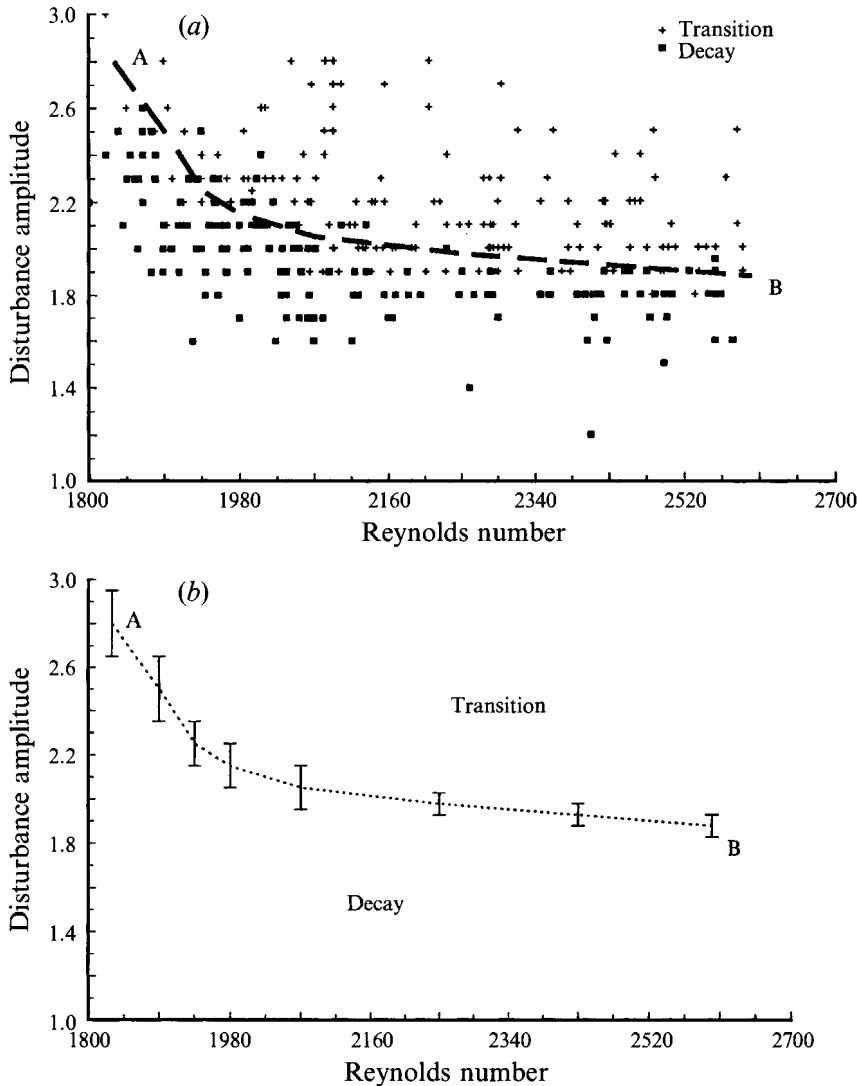


FIGURE 11. (a) Outcomes of experiments using a single-jet disturbance at constant drive speed,  $\omega = 0.409 \text{ s}^{-1}$ , as a function of disturbance amplitude and  $Re$ . (b) Schematic diagram of the results presented in (a). In both cases the dashed line AB is drawn to guide the eye to the critical amplitude.

#### 4.1. Single-jet disturbance

The disturbance used in the first set of experiments was a single jet injected orthogonally into the main flow at a distance  $70D_p$  from the pipe inlet through a 2 mm diameter hole. In each of the experiments, the fluid in the supply tank was allowed to settle for a period of 30 minutes between repetitions. It was found by trial and error that this time was sufficient for all observable motions in the tank to decay. The amplitude of the disturbance was determined by the displacement of the injection mechanism alone, since the drive speed of the associated motor was kept constant at a value  $\omega = 0.409 \text{ Hz}$ . At this frequency the maximum velocity of the injected jet is the same order of magnitude as the main flow and the pulse length is short enough to approximate to a localized disturbance. In fact it corresponds to a peak  $Re \approx 600$

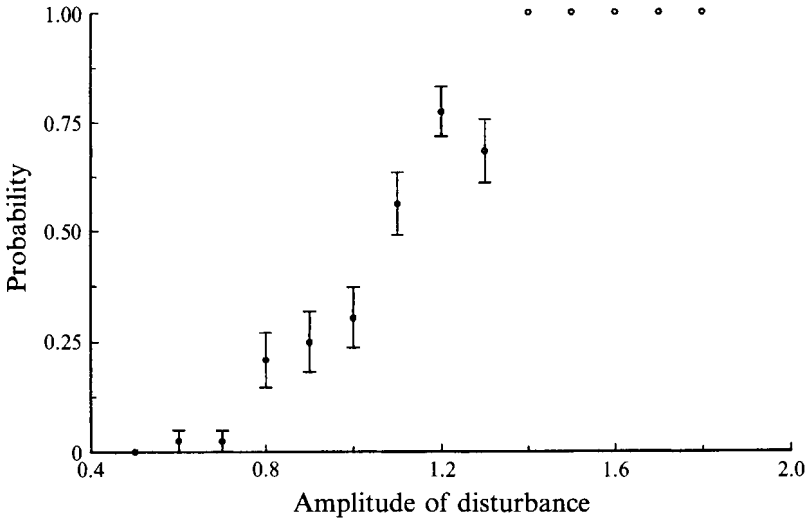


FIGURE 12. Probability of transition for single-jet disturbance at  $Re = 2260$ ,  $\omega = 0.409 \text{ s}^{-1}$ .

based on the diameter of the jet. The outcome of the experiment, i.e. whether transition had occurred or not, was observed  $100D_p$  downstream of the disturbance using flow visualization. This method of observation was chosen for its simplicity after we had established its reliability. Also, the location of the observation station was selected on the basis that fully developed puffs or slugs were readily identifiable there.

We present the results of this part of the experiment in figure 11(a) where we display a plot of the outcome of a particular realization as a function of  $Re$  and disturbance amplitude. The plus signs represent a run where transition occurred and the solid squares one where there was no transition. This figure has been constructed from data obtained in over 500 realizations of the experiment. It can be seen that there are two quite distinct regions. To the right and above the bold dotted line labelled AB most of the runs produced transition while to the left and below this line the initial disturbance decayed before the observation point was reached. We show a schematic representation of these results in figure 11(b) to try and clarify the issue. The error bars indicate the range of amplitudes within which either outcome is possible. This point is explained in more detail below.

For the range of amplitude of disturbances shown in figure 11(a), the ratio of the mass flux of the jet to the unperturbed pipe flow ranges from approximately 1.2% to 2.0%. Other runs of the experiment were performed with amplitudes of perturbation much higher or lower than those shown in figure 11(a) and these resulted in transition or decay in agreement with the displayed results.

The above results suggest that there is a critical finite amplitude of disturbance required to cause transition. The line AB in figure 11(a) has been drawn to guide the eye since there is not a sharp divide between the two possible outcomes. This uncertainty at the boundary between the two regions of figure 11(a) was investigated by setting a constant Reynolds number of  $Re = 2260 \pm 20$  with a constant drive frequency as before. Then at least 40 runs of the experiment were performed at several values of amplitude in the region near the 'critical' threshold. We show the outcome of these experiments in the form of the probability of transition as a function of disturbance amplitude in figure 12. The errors bars denote the expected variance of a set of experimental trials which can be represented by a binomial distribution with the

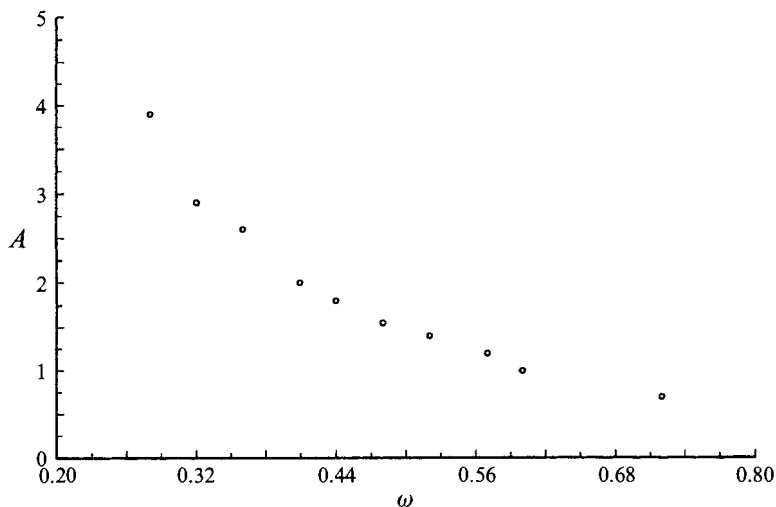


FIGURE 13. Variation of critical disturbance amplitude,  $A$ , against drive speed,  $\omega$  at  $Re = 2200$  for the single-jet disturbance.

measured probability of transition. The results show that the transition is reasonably sharp with an approximate error of  $\pm 11\%$  on the amplitude for a probability of transition of 0.5.

The variation of the critical amplitude of disturbance as a function of the injection drive speed,  $\omega$  (see §2), at constant  $Re$  is shown in figure 13. As might be expected the amplitude required to cause transition decreases as the drive speed increases. However, there does not appear to be any simple relationship based on the maximum mean disturbance velocity or the total mass flux added to the flow. The value of  $\omega$  chosen for the majority of the experiments is in the range where there is least sensitivity in the critical amplitude and for the practical reasons of jet speed and duration discussed above.

#### 4.2. Six-jet disturbance

The six-jet disturbance was injected at the same distance along the pipe as the single jet and the same experimental procedure as discussed above was followed. The drive speed was again kept constant at  $\omega = 0.409$  Hz and a series of runs were performed at various combinations of  $Re$  and disturbance amplitude as before. The outcome of each experiment was observed at a position  $100D_p$  from the disturbance inlet using flow visualization.

The results are shown in figure 14 as a plot of the outcome of each experiment where again the symbols  $+$  and  $\blacksquare$  indicate transition or a decayed disturbance respectively. There is once again a marked boundary between those amplitudes of disturbance which cause transition and those which do not. The absolute value of the disturbance required to produce transition is, in general, lower than that in the case of the single jet. However, the order of magnitude of the disturbance strength is the same and, importantly, the qualitative structure of the finite-amplitude stability curve is retained. This result is somewhat surprising since the fluid is now injected symmetrically and the jets of fluid are directed azimuthally around the walls of the pipe so that the disturbance enters slow-moving fluid and adds a component of swirl to it. One immediate conclusion is that the transition process seems to be insensitive to the particular form of the added disturbance.

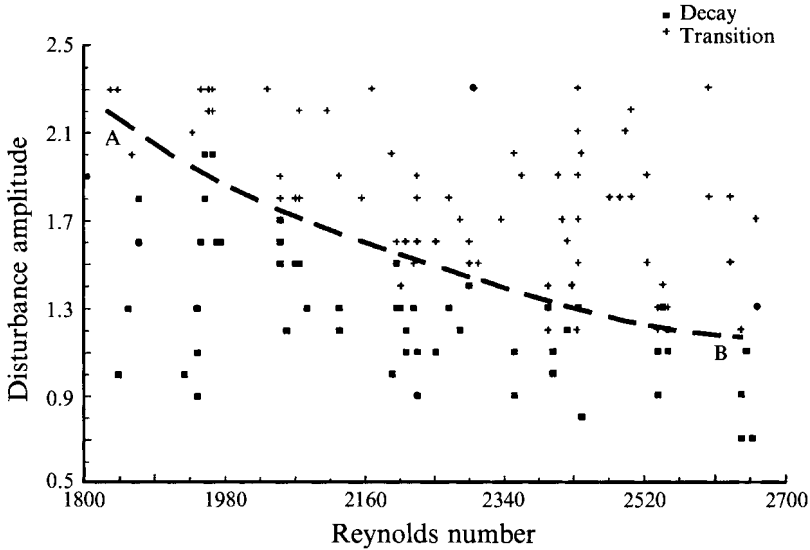


FIGURE 14. Outcomes of experiments using the six-jet disturbance at constant drive speed,  $\omega = 0.409 \text{ s}^{-1}$ , as a function of disturbance amplitude and  $Re$ . The line AB is drawn to help identify the critical amplitude.

#### 4.3. Push-pull disturbance

In the experiments described in the previous two subsections the introduction of a disturbance has added a very small fraction to the total mass flux of the flow and, in principle, its effects are present at all points in the fluid since it is incompressible. Therefore, a third disturbance configuration was designed whereby the net mass flux added to the flow is zero and thus the disturbance is localized. Here the disturbance was created by the six-inlet configuration described above but now with an arrangement of pipes and pumps such that fluid was injected alternately through three of the inlets and sucked out of the other three, i.e. adjacent jets push or pull. The experiments were performed at constant drive speed with the disturbance generator at the same location along the pipe as in the six- and single-jet cases. The outcomes of the experiment are plotted as a function of  $Re$  and disturbance amplitude in figure 15 where AB is again drawn to guide the eye. The coverage is less extensive than in the six- and single-jet cases but again the curve which denotes the boundary between the region where transition occurs and where the disturbance decays is qualitatively the same as above. The absolute value of the disturbance required to cause transition at a given  $Re$  is lower than in the previous two cases but it is of the same order of magnitude. These results provide further evidence for the insensitivity of the transition processes to the particular disturbance geometry.

#### 4.4. Suction disturbance

The final sequence of disturbance experiments were carried out with a single-inlet suction device, i.e. the reverse of the single jet. All of the experiments reported here were confined to a single  $Re$  value of 2260. It was found that the level of disturbance required to cause transition in this case was vastly greater than in any of the other configurations. In particular, it was not possible to cause transition using the drive setting employed in all the other experiments even at the largest available amplitudes. Thus we had to increase the drive frequency to values of  $\omega$  greater than 0.6 Hz before transition could be induced. At  $\omega = 0.75 \text{ Hz}$  the amplitude required to cause transition

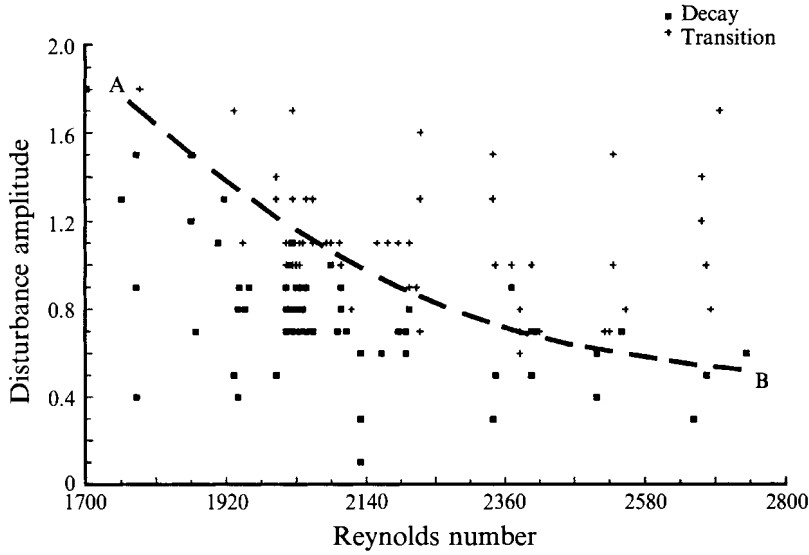


FIGURE 15. Outcomes of experiments using the push-pull disturbance at constant drive speed,  $\omega = 0.409 \text{ s}^{-1}$ , as a function of disturbance amplitude and  $Re$ . The line AB is drawn to guide the eye to the critical amplitude.

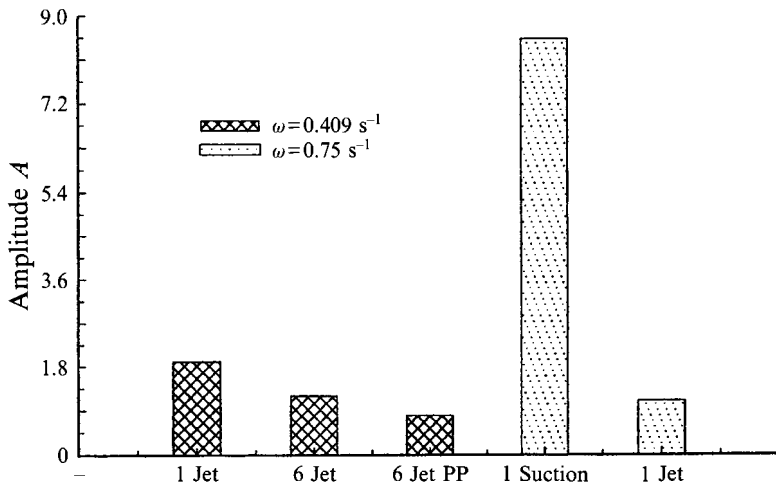


FIGURE 16. Comparison of critical amplitudes required to cause transition for the different disturbance configurations. The line AB is drawn to help identify the critical amplitude.

at  $Re = 2260$  was found to be  $A \approx 8.5$ . We show in figure 16 a plot of the critical amplitude of disturbance required to cause transition at a fixed  $Re$  of 2260 for all four types of perturbation. It may be seen that the amplitude required in the suction experiment is an order of magnitude greater than required for a single jet at the same frequency of drive. It is also the same order greater than either the six-jet or push-pull systems when they were set to  $\omega = 0.409 \text{ Hz}$ .

#### 4.5. Higher Reynolds numbers

The next phase of the experiment consisted of a study of the transition process at higher values of the Reynolds number. These were performed using the six-jet disturbance at the fixed values of  $Re = 4200, 6600$  and  $9900$ . At the highest value of  $Re$  the flow is only

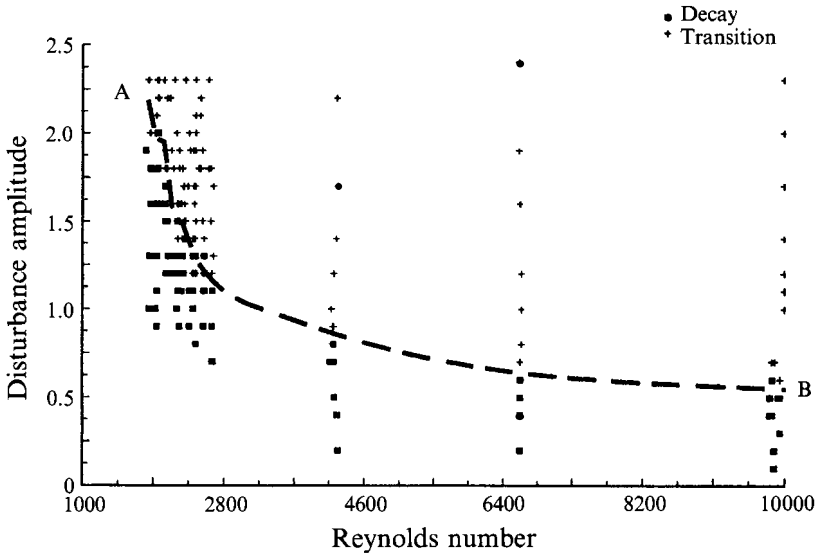


FIGURE 17. As figure 14 except the range of  $Re$  is extended up to  $Re = 10000$ .

84% developed at the disturbance injection point. The drive speed was set to  $\omega = 0.409$  Hz as in the earlier six-jet studies and a comprehensive set of experiments were performed by varying the amplitudes of disturbances. The state of the flow was measured using LDV in this set of experiments. It was again found that there is a critical amplitude of disturbance required to cause the production of a WC73 slug. We show these new results in combination with those discussed above for the case of  $Re < 2700$  in figure 17. There it can be seen that the new results are consistent with the earlier set in that transition occurs at lower disturbance amplitudes as  $Re$  increases. However, the curve only asymptotes towards the zero amplitude limit. Hence, the magnitude of disturbance required the cause transition at  $Re \approx 10000$  is not particularly small when compared with that required to cause transition at  $Re \approx 2500$ . Thus we speculate that it is the inlet disturbances which are crucial in determining the stability of pipe flow in less well-controlled conditions. This observation is in accord with that of Pfenniger (1961) who managed to maintain Poiseuille flow at  $Re$  approaching  $10^5$  in highly controlled experiments.

## 5. Growth of disturbances

We have demonstrated so far that transition can be initiated in a repeatable manner when a prescribed disturbance is introduced into the flow. We now wish to investigate the evolution of the localized injected disturbances as they develop downstream into recognizable turbulent structures. In addition, we wish to see if it is possible to differentiate between those which grow into turbulent puffs and slugs and those which decay. We show in figure 18 a set of flow visualization pictures of the injection of a single-jet disturbance where the injected fluid is dyed black. The top sequence of photographs in figure 18 are of the case where transition results downstream and the bottom set of photographs are of a jet-initiated disturbance which decays. The photographs were taken with an interval of 0.2 s between exposures. It can be seen that over the spatial coverage of these photographs ( $\approx 5D_p$ ) it is very difficult to distinguish

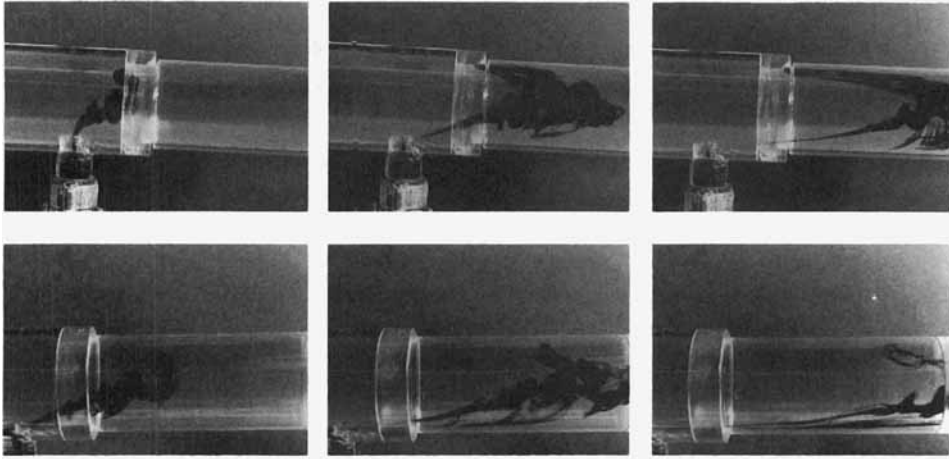


FIGURE 18. Photographs of a single jet close to the disturbance inlet. Top three: transition observed downstream. Bottom three: Disturbance decays away downstream.

between the disturbance which causes transition and the one which decays. This is also true in the case of the six-jet disturbance but this proved to be very difficult to photograph and so we have not displayed the results.

The on-axis streamwise velocity component of the flow was also measured using LDV at a spatial location very close to the disturbance inlet. These results are shown in figure 19 as an ensemble of velocity time records taken  $2D_p$  from the jet disturbance. Both sets of records show that the effect of the jet disturbance is not felt at  $2D_p$  until a finite time has elapsed after the injection. This was found to be true even for the largest values of  $A$  and  $\omega$  used and thus the disturbance can be considered as a localized event. The first motion indicated on the LDV traces shows a small-amplitude long wave which presumably is a precursor to the weak oscillation which forms ahead of the turbulent puff downstream. The only obvious differences between the disturbances which lead to a puff (figure 19*a*) and the ones which decay (figure 19*b*) is that the time series shown in figure 19(*a*) appear to contain more low-frequency components and are approximately 50% longer than their counterparts in figure 19(*b*). Thus, in these very early stages of development, the differences between the two cases are not particularly striking and we can only conclude that the transition process involves more subtle effects.

The latter stages of the development process were next investigated using reflective flakes as the flow visualization agent. Slits of light were placed at various stations along the pipe length to try and identify the spatial position at which it becomes possible to distinguish between a decaying and a growing disturbance. It was found that a definite difference could be observed at spatial positions in the range  $(20-40)D_p$  from the disturbance inlet. We show in figure 20(*a*) a sequence of photographs taken at a position  $35D_p$  from the single-jet disturbance with  $A = 2.1$  and  $Re = 2279$  for the main flow. The photographs were taken 3.9 s after the injection of a disturbance with interval between exposures set to 0.6 s. The flow was illuminated by a sheet of light which had a width of 3–4 mm in a plane containing the pipe axis and orthogonal to the viewing angle. The sequence may be compared directly with that shown earlier in figure 6 where we displayed a typical example of a developed puff. It can be seen that the puff is already quite well-developed by  $35D_p$  from the disturbance inlet.

Next we show in figure 20(*b*) a sequence shot at the same position and  $Re$  used in

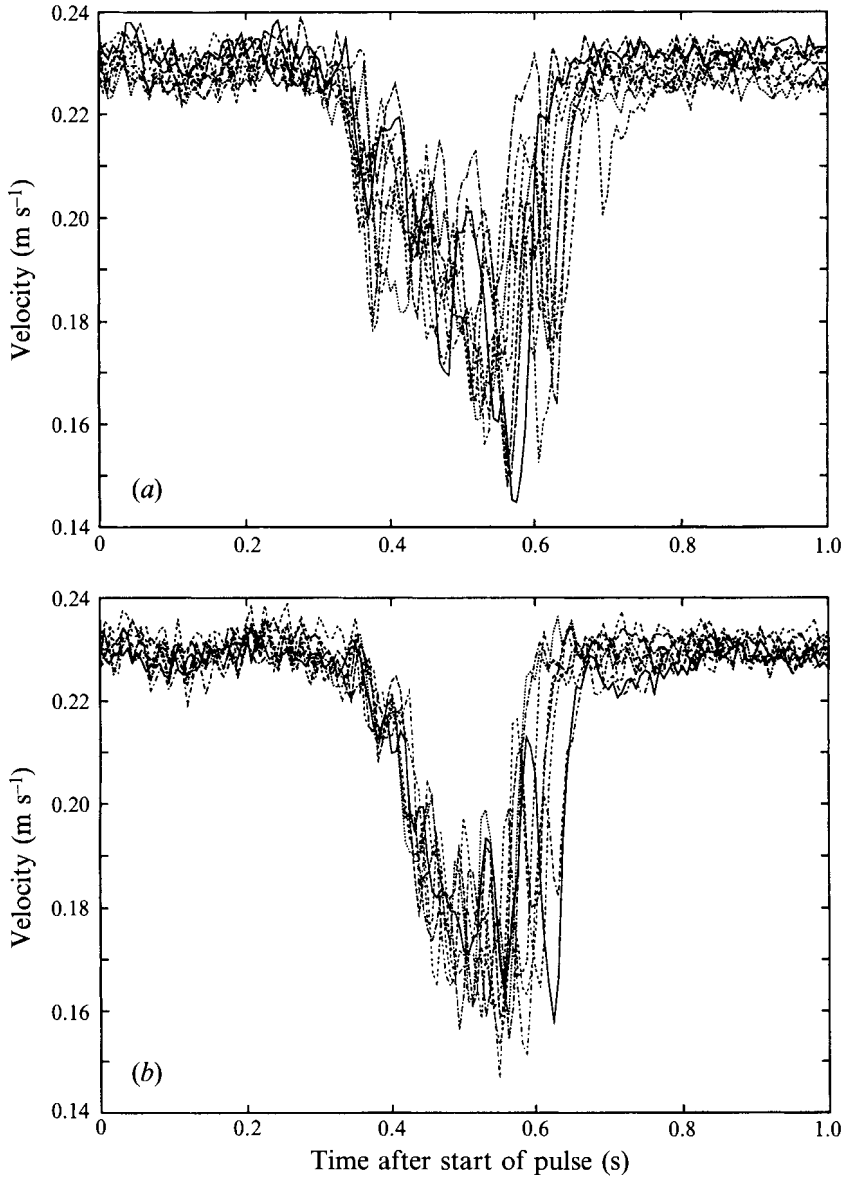


FIGURE 19. Velocity time traces measured  $2D_p$  from the single-jet inlet. (a) Disturbances that cause transition. (b) Disturbances that decay downstream.

the sequence shown in figure 20(a) but now the disturbance amplitude is set to  $A = 1.4$ . In this case there is no obvious puff-like structure nor evidence for turbulence. Instead we see a slowly changing wave-like structure which is approximately  $5D_p$  in length and is a decaying remnant of the injected disturbance. Further insight into the decay process can be gained by comparing the sequence shown in figure 20(b) with the photograph shown in figure 20(c). In the latter case, the photograph was taken close to the disturbance inlet at the same values of  $Re$  and  $A$  as used in figure 20(b), but 0.6 s after the injection began. The disturbance is spread over the whole tube diameter upstream but has decayed to a narrow core region when it reaches the downstream location.

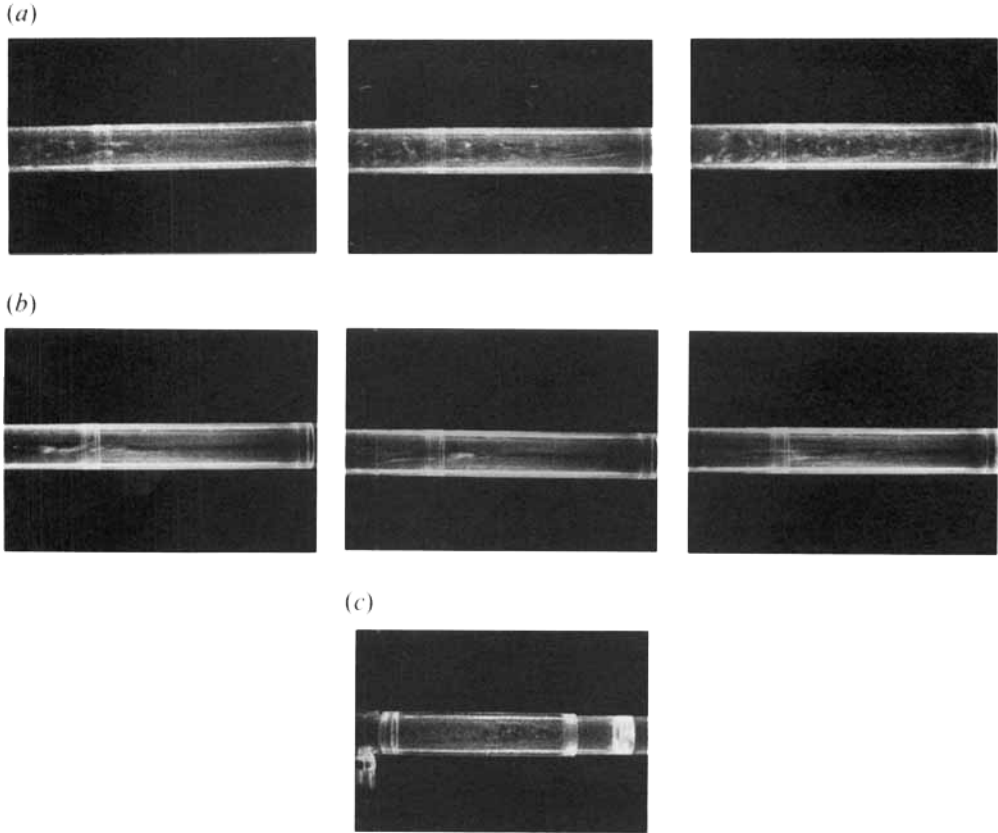


FIGURE 20. (a) Transition flow photographed  $35D_p$  from the disturbance at  $A = 2.1$ . (b) Decaying disturbance photographed  $35D_p$  from the disturbance at  $A = 1.4$ . (c) As (b) but photographed  $2D_p$  from the disturbance.  $Re = 2279$ .

Further insight into the intermediate stages of the transition process can be gained by reverting to the inkjet visualization technique in combination with the six-jet disturbance. In this case, the angle at which the jets enter the flow enables the ink to remain visible for a longer distance downstream than with the single jet where most of the marked fluid is dispersed by the faster-moving fluid in the main flow.

The sequences shown in figure 21 were taken at a downstream distance of  $22D_p$  from the six-jet disturbance with  $Re$  fixed at 2260 and the interval between exposures set to 0.4 s. The set of photographs presented in figure 21(a) show a disturbance initiated with  $A = 1.6$  which was observed to develop into a puff  $90D_p$  downstream of the inlet. One clear feature, present in all the photographs in this sequence, is that the marked fluid has been drawn into the flow on the central axis of the pipe. Also the photographs towards the end of the sequence show a distinct turbulent region which is sharply separated from the upstream laminar flow following on behind. The boundary between the two flow regimes is clear, particularly in the last two exposures. One conclusion which may be drawn from these flow visualization photographs is that the turbulence arises during the early part of the injected disturbance when the jets have highest mean flow speed (recall that the disturbance speed rises sharply before falling linearly as shown in figure 3 b). Thus the ink injected with the slowest mean speed in the final phase of the perturbation is drawn along the walls of the tube by the laminar Poiseuille flow.

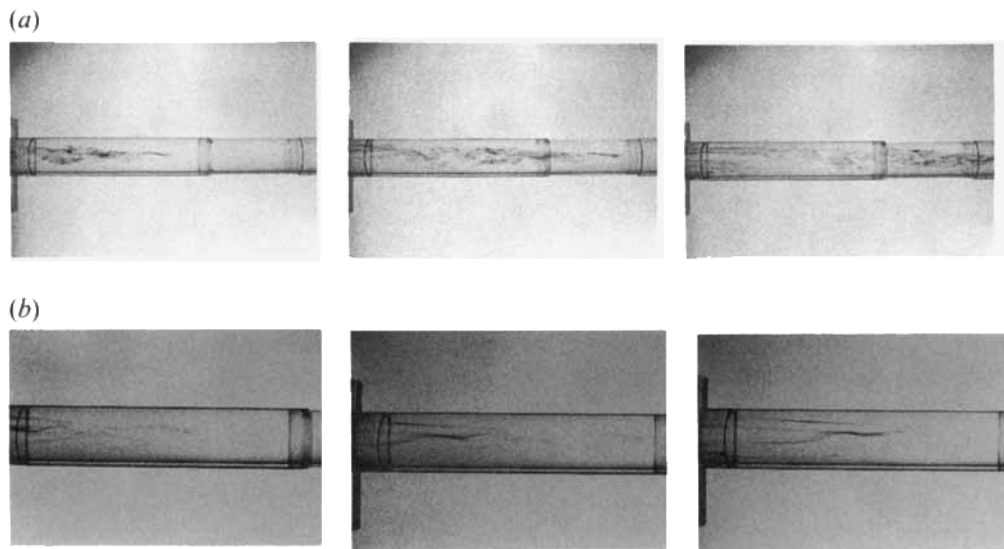


FIGURE 21. Tracer flow visualization photographs of flow  $22D_p$  from the six-jet disturbance inlet. (a) Transition flow; (b) Decaying disturbance.

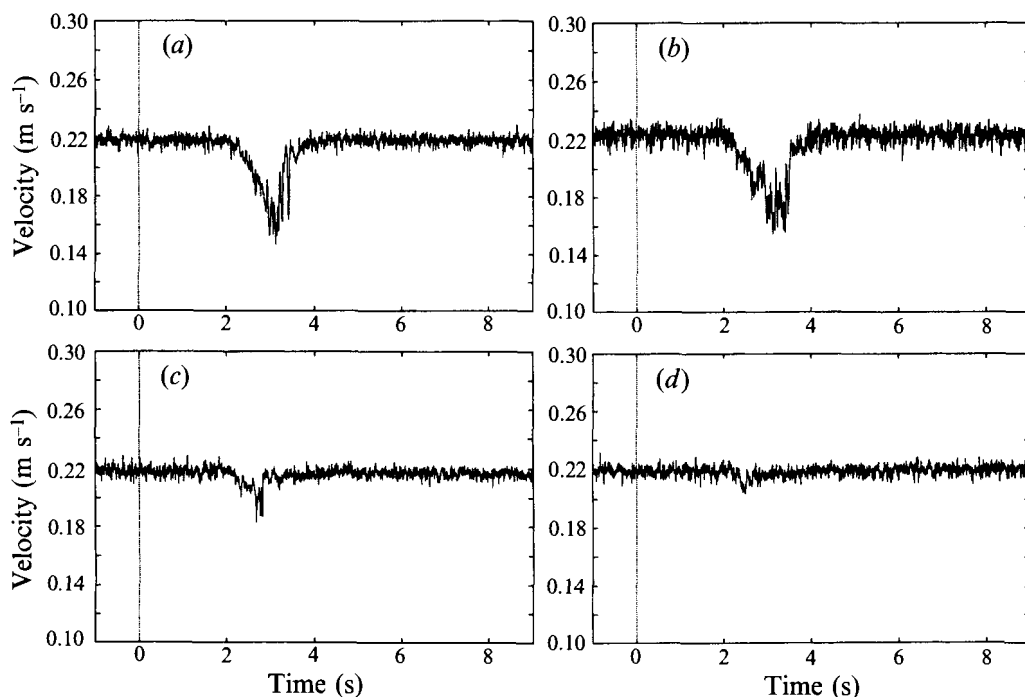


FIGURE 22. LDV velocity time traces measured on the pipe axis  $22D_p$  from the six-jet disturbance inlet. (a, b) Flows where transition is observed downstream,  $A = 1.5$ . (c, d) Decaying disturbances,  $A = 1.2$ ,  $Re = 2263$ .

The sequence of photographs shown in figure 21(b) were taken with the same conditions as above but now the injected disturbance has an amplitude  $A = 1.2$ . It was observed that this disturbance had completely decayed when observations were made at  $90D_p$  downstream. As in the case discussed above we can again see a slowly

changing wave-like structure at the centre of the pipe but now there is no evidence for the presence of turbulence. Thus the contrast between the two sequences shown in figures 21(a) and 21(b) suggests that a difference between a disturbance which grows into a turbulent puff and one which decays can be discerned within  $25D_p$  of the point of injection.

The latter conclusion is also supported by LDV measurements made at the same spatial location as above. We show in figure 22 four axial velocity time series measured on the central axis of the pipe. In the case of the traces presented in figure 22(a, b) where  $A = 1.5$  and transition was observed downstream, the features of a rudimentary puff are clear. In contrast, the traces shown in figure 22(c, d) where  $A = 1.2$  and no transition was observed, the disturbance has almost completely decayed by this station.

In summary, we can conclude that transition is initiated close to the point of injection. Also, those disturbances which do not cause transition have noticeably decayed within  $25D_p$ . This is true even for disturbances which are very close to the critical amplitude. It is this latter feature which we believe gives us strong evidence that the phenomena we observe at distances of  $100D_p$  from the disturbance inlet are not transient events. Thus in almost all cases the observations made at  $100D_p$  from the injection point detect either a recognizable transition event or the disturbance has dissipated to such an extent that the perturbation cannot be detected either by flow visualization or the LDV system. Some exceptions to this rule occur infrequently ( $< 1\%$  of the time) at values of  $A$  close to the critical amplitude. Here a wave-like flow was sometimes seen and it was very difficult to tell whether it was decaying or not. This flow was only rarely seen using flow visualization and its effect was so weak that it was not readily distinguished from laminar flow using the LDV system. We believe that these latter observations may be indicative of a neutrally stable flow which is generated very occasionally.

## 6. Response of the flow at $Re < 1800$

In the overview of the general properties of the transitional flow presented in §3 we noted that there is a value of  $Re$  below which no turbulent structures can be sustained. This result is consistent with the results of previous workers (WC73; WSF75; Lindgren 1958). In the finite-amplitude stability curves (figures 11, 14 and 15) obtained for three different disturbance geometries it can be seen that the amplitude required to cause transition increases rapidly as  $Re$  decreases towards 1800. These results suggest that the amplitude rises asymptotically to a large value at some finite value of  $Re$ . In order to investigate this feature we performed several experiments with the six-jet disturbance at larger values of  $A$  than those used to construct figure 14. The experiments were performed using the LDV system to measure the downstream outcome of a disturbance injected upstream. In some of the runs flow visualization particles were added to the fluid in addition to using the LDV system. This degrades the LDV signal quality but the main features in the flow are visible by both means.

We show in figure 23 some example time series obtained from a set of runs of the experiment at  $Re = 1760$  where a six-jet disturbance with  $A = 3.7$  was used. At these  $Re$  and large  $A$  we observed the flows shown in figure 23(a, b) which have velocity time histories reminiscent of turbulent puffs at higher  $Re$ . Visually the flow is indistinguishable from a short turbulent puff with the characteristic sharp interface between the laminar and disordered region. In contrast, the flows whose time traces have the form of long shallow perturbations on the main flow shown in figure 23(c, d) are reminiscent of the decaying disturbances shown in the previous section for higher

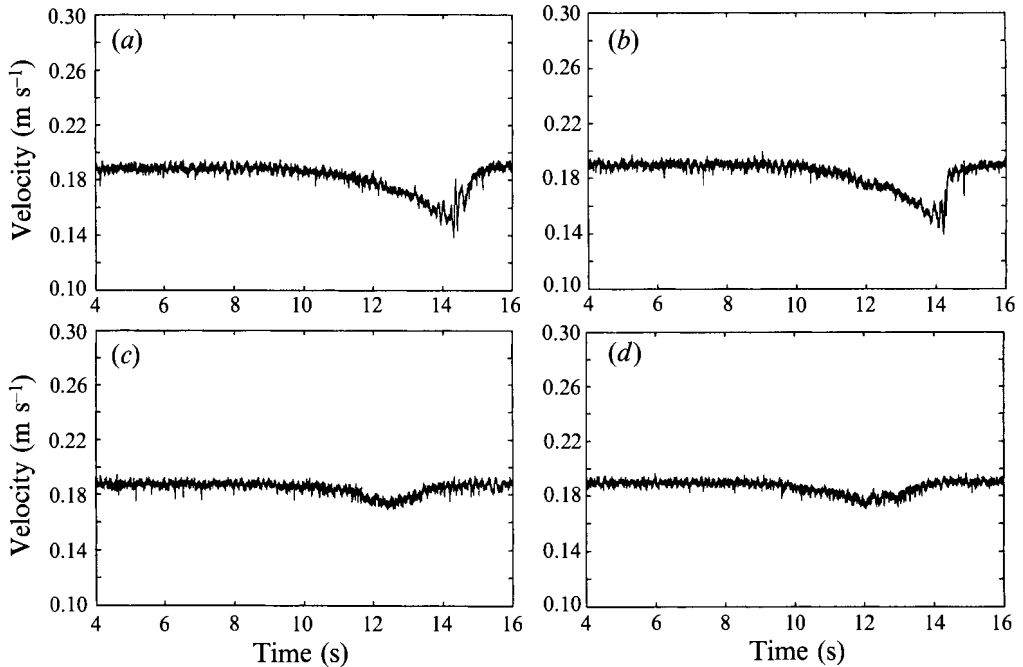


FIGURE 23. LDV measurements of disturbances  $100D_p$  from the disturbance inlet at  $Re = 1760$ . (a, b) Flows where transition has occurred. (c, d) Decaying disturbances.

$Re$ . The spatial decay length for disturbances close to the critical amplitude is much longer than at higher  $Re$  but this may be because the absolute size of the decaying disturbance is greater. At even lower  $Re$  the critical amplitude is less well defined. We can therefore conclude that it soon becomes impossible to sustain disordered motion in the flow even when the amplitude of the disturbance is made large.

## 7. Measurements of the turbulent/laminar interface

When observing the transition to turbulence in a pipe by means of flow visualization, the most striking feature is the apparent abrupt change as the turbulent/laminar interface is advected through the field of view of the observer. The sequences of still photographs presented above fail to capture some of the features of the interface region which are readily seen by direct observation during repetitions of the experiment. In particular, the interface has dynamic features which have time scales comparable with the shortest interval between exposures achievable by the camera system (0.2 s). These details are thus often missed in the captured images. Therefore, the LDV system was used to investigate the detail of the relaminarization phase at the tail of the puff.

All of the experimental results discussed here were taken at constant values of the experimental parameters,  $Re = 2490$  and  $A = 1.8$ , and an example of the results is presented in figure 24. This amplitude of disturbance guaranteed a transition event for every run of the experiment. It can be seen in figure 24(a) that just before the sharp tail of the puff advects past the measurement point there is a drop in the axial velocity component which appears as a spike in the velocity time series. This indicates that there is an ‘incursion’ or ‘island’ of fluid within the tail of the puff which has the velocity of the laminar flow. We have highlighted this feature in figure 24(b) by expanding the

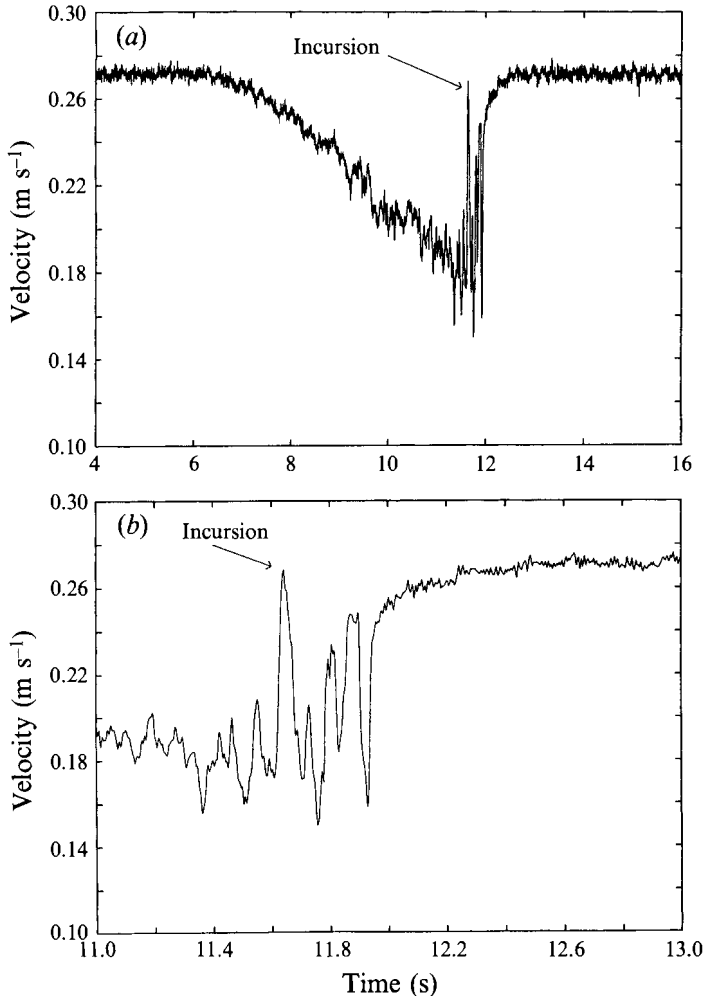


FIGURE 24. LDV recordings at  $Re = 2491$  showing (a) example of 'incursion' in an equilibrium puff flow, (b) expanded time scale close to the rear interface.

time scale so that the incursion may be seen more clearly. The time duration of this incursion is approximately 50–100 ms which implies that it has a length scale of  $(0.5-1) D_p$  based on the laminar flow speed. It can also be seen in this instance that there are other smaller waves between the largest incursion and the laminar region. However, this is not typical and usually there is just one incursion, followed by disordered motion and then the final interface. These incursion events have magnitudes which are much larger (approximately 8–10 times greater) than the noise level of the LDV system and the velocity gradient implied by the measurement is well within the range which can be resolved by the LDV signal processing device (TSI IFA550). Also they only occur in approximately 20–30% of turbulent puff observations, and an example of a time trace where there is no evidence for incursion may be seen in figure 7.

This type of incursion event was noted by Wygnanski and his co-workers (WSF75, figure 18) who interpreted the observation as evidence for an incipient splitting of the turbulent puff. They then used this mechanism to explain why two turbulent puff structures occasionally arose from a single pulse disturbance. However, in our system

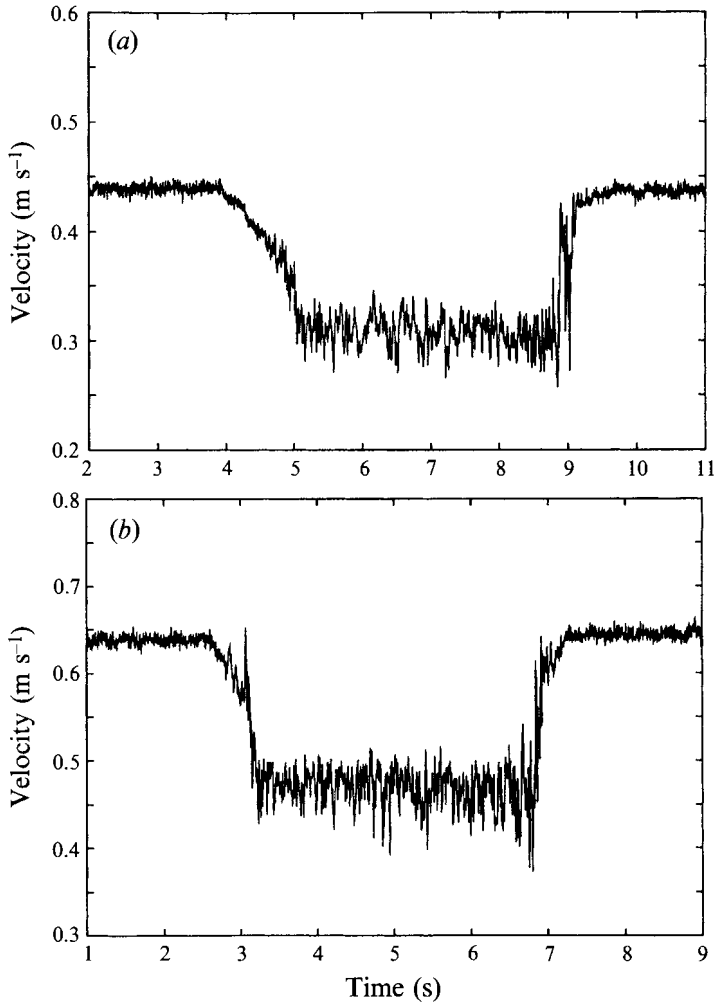


FIGURE 25. LDV recordings showing examples of 'incursion' in slug flows.  
(a)  $Re = 4260$ , (b)  $Re = 6650$ .

we have not observed splitting of turbulent puffs even when the disturbance injection point was moved  $50D_p$  towards the pipe inlet. This could imply that splitting does not occur in our system because of the relatively short spatial distance ( $< 170D_p$ ) we have available to observe downstream of the disturbance injection point.

The incursion phenomena were also observed at higher Reynolds numbers in the turbulent slug regime. We show in figure 25 velocity time records measured at  $Re = 4270$  (25a) and at  $Re = 6650$  (25b). At the lower Reynolds number the incursion is only found at the rear interface. However, in the higher  $Re$  case where the slug has the generic (high- $Re$ ) sharp front and rear interfaces it can be seen that there are incursions of laminar fluid at both ends. The front interface in this case is moving with a speed  $1.4U_m$ . It must be recalled that these are only single-point measures of one velocity component, thus it is difficult to make quantitative assessments of the spatial dimension or the time duration of these incursions. However, since incursions are found in 20–30% of the records of puff flows, but are less frequently observed in the

slug flows, this suggests that the duration and frequency of the incursions are functions of  $Re$ . The incursions could also be related to the 'islands' observed at the rear interface of turbulent puffs using high-speed photography and dye flow visualization by Bandyopadhyay (1986).

Our interpretation of the above features is that there is an eddy or wave structure at the rear interface which cyclically entrains the faster-moving fluid in the central axis region of the pipe. The excess energy from this faster-moving fluid is then dissipated by turbulence production, as the fluid is swept out towards the pipe wall thereby maintaining mass flux balance. An alternative explanation is that the interface is not a constant feature but breaks and remakes itself intermittently. Also the 'turbulent' or disordered fluid is moving at a speed  $U_m$  whilst the fluid in the laminar axis region is moving at speeds up to  $2U_m$ . Thus the disordered fluid could be considered as a slow-moving barrier which can only be overcome when enough momentum has built up in the region around the central axis. Again the faster fluid would dissipate energy which would then sustain the turbulent region.

In slug flows, where the mean flow speeds are higher, one might expect the turbulence production to be greater and hence the disordered region would grow in spatial extent causing the front interface to travel at speeds greater than  $U_m$ . Thus, once the turbulent slug has developed entrainment could take place at both interfaces.

## 8. Discussion and conclusions

We have performed a systematic study of the transition to turbulence at constant  $Re$  and have shown that the general features associated with the transition to turbulence in our constant-mass-flux rig are the same as have been previously reported for pressure-driven systems. Indeed, a comparison of flow visualization and LDV measurements with previous studies reveals qualitatively the same flow features and quantitative agreement on the propagation speed and spatial growth of the turbulent structures. These findings cast doubt on the claim that the sharp relaminarization interfaces are due to a reduction in Reynolds number caused by the presence of patches of turbulence.

An equally important conclusion which may be drawn is that a critical amplitude of disturbance is required to cause transition and it is a slowly decreasing function of  $Re$  beyond  $Re \approx 2100$ . The experiment is repeatable over a wide range of Reynolds numbers and we have shown that a sustained transition is not possible for  $Re < 1760$  even with very large-amplitude disturbances. Moreover the quantitative repeatability of the results, as highlighted for the single-jet disturbance in figure 12, is somewhat of a surprise in the light of the sensitivity to initial conditions found in nonlinear systems. We might expect the outcome of any given experiment to vary such that transition would be found to occur over a wider range of disturbance amplitudes, given the complex detail of the perturbation. Furthermore, when the qualitative nature of the disturbance is changed from orthogonal to azimuthal jets we find the same repeatable behaviour and only the absolute value of the critical amplitude is altered.

The finite-amplitude stability curve approaches the infinite Reynolds number limit asymptotically since at  $Re \approx 10000$  the critical amplitude required for transition is the same order as that required at  $Re \approx 2500$ . This is in accord with theory since it is known that Poiseuille flow is linearly stable. In addition, the magnitude of the critical amplitude is roughly the same for the three very different types of perturbation with the lowest value found in the push-pull system. This configuration will generate more shear in the flow near the wall and could well promote local instabilities.

One qualification we must highlight about our work concerns the short length of the pipe used in the experiments. Ideally one would like to make the pipe long enough to be able to inject the disturbances into 100% developed flow, and observe their evolution, but this was not possible owing to practical considerations. In §2 we show that the pipe flow at  $Re \approx 2200$  is 94% developed at the spatial location where the disturbances are injected into the flow, and that the profile is close to the mathematical idealization of fully developed Poiseuille flow. The range of experiments we have performed suggests that the phenomena we observe do not depend on the details of the velocity profile in the centre of the tube. At  $Re \approx 10000$  we still need a finite-amplitude disturbance of the same order of magnitude as that needed to cause transition at  $Re \approx 2200$ , despite the flow being only 84% developed at the injection point in the higher- $Re$  case. It is our contention that once a viscous layer has developed over most of the pipe then the finite-amplitude perturbation required to trigger the onset of disordered motion is insensitive to the details of the core flow. This is unlike the situation at the entrance to the pipe where boundary layer concepts are more appropriate and small-scale perturbations can cause transition.

We speculate that the existence of a critical finite-amplitude stability curve may imply that there are other flow states which are disconnected from the laminar Poiseuille flow. Thus these new solutions cannot be reached by a continuous variation of the parameters which govern the flow. Solutions of this type have been reported previously in different fluid problems: Cowley & Smith (1985) for Poiseuille–Couette flow, Anson, Mullin & Cliffe (1990) for the Taylor–Couette problem and Nagata (1990) for plane Couette flow. The latter problem is, like circular Poiseuille flow, linearly stable. The disturbance could be thought of as providing a large enough perturbation to propel the flow from the basin of attraction of the trivial Poiseuille state into a new disordered state. A future direction of our research will be to investigate this possibility by establishing transition and then reducing the Reynolds number in a controlled way. This should allow us to establish the form of the disconnected state, if it exists as a steady flow, and this could then provide the basis for a numerical stability analysis.

The spatial growth of the disturbances into recognizable turbulent structures appears to be a rapid process since growing and decaying disturbances with amplitudes close to the critical values can be differentiated from one another within  $(20\text{--}30) D_p$  of the disturbance inlet. This finding seems to be at odds with the results of many previous studies and we can only speculate that it occurs because we are injecting disturbances into a more developed flow field. It also suggests that if the basic flow is unstable to a finite-amplitude wave-like perturbation, then the scale size would be of order a few pipe diameters. In fact, some experiments have been conducted by Landman (1990) to try to find stable helical states, but each initial helical flow decayed back to Poiseuille flow.

It is known that, once established, the spatial extent of the disordered region of puff flows at low  $Re$  does not change with distance downstream and hence they were said to be in an equilibrium state by WSF75. Thus we speculate that the waves which are often observed ahead of the disordered region may be decaying remnants of the wideband turbulence in the main body of the puff. However, in the case of slug flows, the front face of the disordered region proceeds faster than the mean flow so that there would not be enough time for a wave to be established. The observation of incursions in both turbulent puffs and turbulent slugs suggests that there may be a common mechanism for maintaining disordered flow in both regimes. Thus a possible future direction of study would be to capture simultaneous multipoint measurements of velocity so that information about the coherence of the time-dependent velocity field

could be obtained. This should be feasible using particle image velocimetry (PIV) (Adrian 1991) which would greatly enhance our knowledge of the whole flow fields associated with these phenomena.

This work was supported by the UK Science and Engineering Research Council under its 'Nonlinear Initiative'. The authors would like to thank Dr Derek Wyatt who designed and built the original flow apparatus and gave a great deal of useful incisive advice. Mr Keith Long augmented the original rig and maintained it during the course of these experiments. We would also like to thank Professors T. B. Benjamin FRS, M. Gaster FRS and R. Narashima for helpful comments.

## REFERENCES

- ADRIAN, R. J. 1991 Particle imaging techniques for experimental fluid mechanics. *Ann. Rev. Fluid Mech.* **23**, 261–304.
- ANSON, D. K., CLIFFE, K. A. & MULLIN, T. 1990 A numerical and experimental investigation of a new solution in the Taylor vortex problem. *J. Fluid Mech.* **207**, 475–487.
- BANDYOPADHYAY, P. R. 1986 Aspects of the equilibrium puff in transitional pipe flow. *J. Fluid Mech.* **163**, 439–458.
- BENJAMIN, T. B. 1978 Bifurcation phenomena in steady flow of viscous fluid. Part 1. Theory. *Proc. R. Soc. Lond. A* **359**, 1–26.
- BERGSTROM, L. 1993 Optimal growth of small disturbances in pipe Poiseuille flow. *Phys. Fluids A* **5**, 2710–2720.
- BINNIE, A. M. & FOWLER, J. S. 1947 A study by a double refraction method of the development of turbulence in a long cylindrical tube. *Proc. R. Soc. Lond. A* **192**, 32–44.
- COLES, D. 1981 Prospects for useful research on coherent structure in turbulent shear flow. *Proc. Indian Acad. Sci (Engng Sci.)* **4**, 111–127.
- COWLEY, S. J. & SMITH, F. T. 1985 On the stability of Poiseuille–Couette flow: a bifurcation from infinity. *J. Fluid Mech.* **156**, 83–100.
- DAVEY, A. 1978 On Itoh's finite amplitude stability for pipe flow. *J. Fluid Mech.* **86**, 695–703.
- DAVEY, A. & NGUYEN, H. P. F. 1971 Finite-amplitude stability of pipe flow. *J. Fluid Mech.* **45**, 701–720.
- DRAZIN, P. G. & REID, W. H. 1981 *Hydrodynamic Stability*. Cambridge University Press.
- FARGIE, D. & MARTIN, B. W. 1971 Developing laminar flow a pipe of circular cross-section. *Proc. R. Soc. Lond. A* **321**, 461–476.
- FOX, J. A., LESSEN, M. & BHAT, W. V. 1968 Experimental investigation of the stability of Hagan–Poiseuille flow. *Phys. Fluids* **11**, 1–4.
- GASTER, M. 1990 The nonlinear phase of wave growth leading to chaos and breakdown to turbulence in a boundary layer as an example of an open system. *Proc. R. Soc. Lond. A* **430**, 3–24.
- ITOH, N. 1977 Nonlinear stability of parallel flows with subcritical Reynolds numbers. Part 2. Stability of pipe Poiseuille flow to finite axisymmetric disturbance. *J. Fluid Mech.* **82**, 469–479.
- JOSEPH, D. D. 1981 Hydrodynamic stability and bifurcation. In *Hydrodynamic Instabilities and the Transition to Turbulence* (ed. H. L. Swinney & J. P. Gollub), pp. 27–76. Springer.
- LANDMAN, M. J. 1990 On the generation of helical waves in circular pipe flow. *Phys. Fluids A* **2**, 738–747.
- LEITE, R. J. 1959 An experimental investigation of the stability of Poiseuille flow. *J. Fluid Mech.* **5**, 81–96.
- LINDGREN, E. R. 1958 The transition process and other phenomena in viscous flow. *Arkiv für Physik* **12**, 1–169.
- MADDEN, F. N. & MULLIN, T. 1994 The spin-up from rest of a fluid-filled torus. *J. Fluid Mech.* **265**, 217–244.
- NAGATA, M. 1990 Three-dimensional finite amplitude solutions in plane Couette flow: bifurcation from infinity. *J. Fluid Mech.* **217**, 519–527.

- PFENNIGER, W. 1961 Transition in the inlet length of tubes at high Reynolds numbers. In *Boundary Layer and Flow Control* (ed. G. V. Lachman), pp. 970–980. Pergamon.
- REYNOLDS, O. 1883 An experimental investigation of the circumstances which determine whether the motion of water shall be direct or sinuous and of the law of resistance in parallel channels. *Proc. R. Soc. Lond.* **35**, 84–99.
- ROTTA, J. 1956 Experimenteller Beitrag zur Entstehung turbulenter Strömung im Rohr. *Ing-Arch.* **24**, 258–281.
- RUBIN, Y., WYGNANSKI, I. J. & HARITONIDIS, J. H. 1980 Further observations on transition in a pipe. In *Laminar-Turbulent Transition; Proc. IUTAM Symp. Stuttgart, FRG, 1979* (ed. R. Eppler & F. Hussein), pp. 19–26. Springer.
- SCHUBAUER, G. B. & SKRAMSTED, H. K. 1947 Laminar boundary layer oscillations and transition on a flat plate. *J. Res. Nat. Bur. Stand.* **38**, 251–292.
- SMITH, A. M. O. 1960 Remarks on transition in a round tube. *J. Fluid Mech.* **7**, 565–576.
- SMITH, F. T. & BODONYI, R. J. 1982 Amplitude dependent neutral modes in the Hagen–Poiseuille flow through a circular pipe. *Proc. R. Soc. Lond. A* **384**, 463–489.
- STUART, J. T. 1981 Instability and transition in pipes and channels. In *Transition and Turbulence: Proc. Symp. at the Mathematics Research Centre, University of Wisconsin-Madison, October 1980*, pp. 77–94. Academic.
- TATSUMI, T. 1952 Stability of the laminar inlet flow prior to the formation of Poiseuille regime. Parts 1 and 2. *J. Phys. Soc. Japan* **7**, 489–501.
- TRITTON, D. J. 1988 *Physical Fluid Dynamics* (2nd edn). Oxford University Press.
- WYGNANSKI, I. J. & CHAMPAGNE, F. H. 1973 On transition in a pipe. Part 1. The origin of puffs and slugs and the flow in a turbulent slug. *J. Fluid Mech.* **59**, 281–351 (referred to herein as WC73).
- WYGNANSKI, I. J., SOKOLOV, M. & FRIEDMAN, D. 1975 On transition in a pipe. Part 2. The equilibrium puff. *J. Fluid Mech.* **69**, 283–304 (referred to herein as WSF75).